Bulletin of the Seismological Society of America. Vol. 61, No. 6, pp. 1589–1623. December, 1971

GENERATION OF SEISMIC WAVES BY EXPLOSIONS IN PRESTRESSED MEDIA

M. Nafi Toksöz, Ker C. Thomson, and Thomas J. Ahrens

ABSTRACT

The mechanisms of generation of seismic waves by an explosion in prestressed media are studied using both field seismograms and controlled laboratory experiments. LRSM seismograms from the underground nuclear explosion BILBY are analyzed to determine the source parameters from the radiated Love and Rayleigh waves. From the normalized amplitudes of Rayleigh waves as well as the Love-Rayleigh amplitude ratios, a composite source consisting of an isotropic explosion and a double couple is synthesized for the explosion and the associated tectonic strain release. From BILBY and other explosions studied by similar techniques, it is found that the tectonic strain energy release strongly depends on the medium properties in the immediate vicinity of the explosion. For "harder" media (such as granite) the tectonic strain energy release and the relative amplitude of Love waves are significantly higher than for softer media such as alluvium. Source-time functions of Love waves associated with the explosions are closer to time functions of earthquakes than to those of explosions.

The mechanisms of the pre-existing strain energy release by explosive sources are studied in two separate laboratory experiments. In a one-dimensional experiment where an explosive source is detonated in a rod stressed in torsion, the *S*-wave amplitudes are found to be linearly proportional to prestrain. In the second experiment, radiation of seismic waves and the near-source phenomena of explosive sources in prestressed plates are studied by photoelastic as well as strain gauge observations. The generation of *S*-waves is greatly enhanced by the prestress condition. It is found that extended cracking (faulting) occurs along directions determined by the prestress field. The transverse (*SH*) waves are generated primarily by the relaxation of the stress field along these cracks. The explosion-generated cavity alone could not account for the radiated transverse seismic energy.

Introduction

Seismic surface and body waves generated by underground explosions and recorded at distant stations quite often show characteristics differing from those of an ideal explosive point source in a homogeneous medium. Most notable among these differences are the presence of Love waves and the azimuthal asymmetry of the Rayleigh-wave radiation patterns. Through numerous studies, it has been shown that the Love waves are produced at the source region, although the exact mechanism of their generation still cannot be clearly defined. The purpose of this paper is to present and interpret data, obtained from underground nuclear explosions and controlled laboratory experiments, on seismic waves generated by explosive sources in stressed media.

There have been a number of studies dealing with the radiation patterns and the generation of *SH*-type seismic waves by underground nuclear explosions (Press and Archambeau, 1962; Brune and Pomeroy, 1963; Aki, 1964; Toksöz *et al.*, 1964; Toksöz *et al.*, 1965; Toksöz, 1967; Kehrer, 1969; Molnar *et al.*, 1969; Tsai and Aki, 1971). In

addition, there are a number of previous theoretical studies on the problems of seismic-wave generation by explosions (Zvolinskii, 1960; Bishop, 1963; Alverson, 1964; Cisternas, 1964; Butkovich, 1965; Archambeau, 1968). Difficulties in describing wave propagation from nuclear explosions arise because of very high stresses involved. In the immediate vicinity of the explosion, shock phenomena dominate, whereas in the far zone, elastic behavior prevails. The transition region is extremely important to the understanding of seismic-wave generation, yet this region is extremely difficult to describe mathematically.

In the description of this complex problem, difficulties arise both in mathematical formulation and from inadequate knowledge of the behavior of geological materials under shock loading. In the zone immediately around the explosion, relatively small volume, hydrodynamic compressible flow equations can be used without major assumptions or approximations. In the zones where the rocks are crushed and cracked, however, neither fluid nor elastic behavior can be assumed, and a semiempirical treatment based on approximations and available data must be followed. If the explosion is placed in a medium where tectonic stresses exist, other complications arise from the stress relaxation around the cavity, the crushed zone, and the zone of numerous shock-induced cracks.

Controlled laboratory experiments can provide some of the information needed for the understanding of seismic-wave generation by explosions in prestressed media. Some experiments have been conducted in the field using explosive sources in soil (Kisslinger *et al.*, 1961). Other model experiments have been carried out in the laboratory using explosive sources in prestressed plates. In these tests, the radiation patterns of seismic compressional and shear waves were observed with various transducers and oscilloscopes (Kim and Kisslinger, 1967; Kisslinger and Gupta, 1963). Most recently, photoelastic techniques have been used to observe wave generation and propagation in prestressed media (Thomson *et al.*, 1969).

In this paper, we will treat, in three steps, the problem of mechanisms of seismic-wave generation by explosive sources in prestressed media. First, we describe the radiation pattern of surface waves from a typical underground explosion at the Nevada Test Site. We determine its source mechanism by using an amplitude equalization scheme. In part two, we describe the results of laboratory experiments in which explosive sources were detonated in plates under different prestress conditions. Here, the mechanisms of seismic-wave generation, crack formation, and source complications were observed using dynamic photoelasticity and high-speed photographic techniques. Finally, we interpret the field observations in light of laboratory findings.

Field Observations

Seismic waves from a large number of the U. S. underground explosions have been well-recorded by Long Range Seismic Measurements (LRSM), World Wide Standard Seismographic Network (WWSSN) and other seismograph stations in North America. LRSM stations provide the best recordings of surface waves in the period range of 10 to 40 sec. Most of the large explosions detonated in relatively hard geological media (granite, tuff) generate Love waves in addition to Rayleigh waves. Two examples of Love waves from explosions are shown in Figures 1 and 2. Explosions in loose alluvium and salt domes, and collapse events following explosions, do not generate a significant amount of Love waves. The main body of this study is devoted to the understanding of the generation of these transverse waves. Some sources that must be considered are: (1) relaxation of the prestressed medium around the explosion-generated cavity, (2)

triggering of an earthquake by the explosion, (3) radiation from explosion-induced cracks in the medium, and (4) a combination of all of these.

In order to resolve this problem, it is useful to first determine the radiation patterns of Rayleigh and Love waves. A group of explosions have been studied using the amplitude equalization method (Toksöz, *et al.*, 1964, 1965; Toksöz, 1967; Kehrer, 1969).

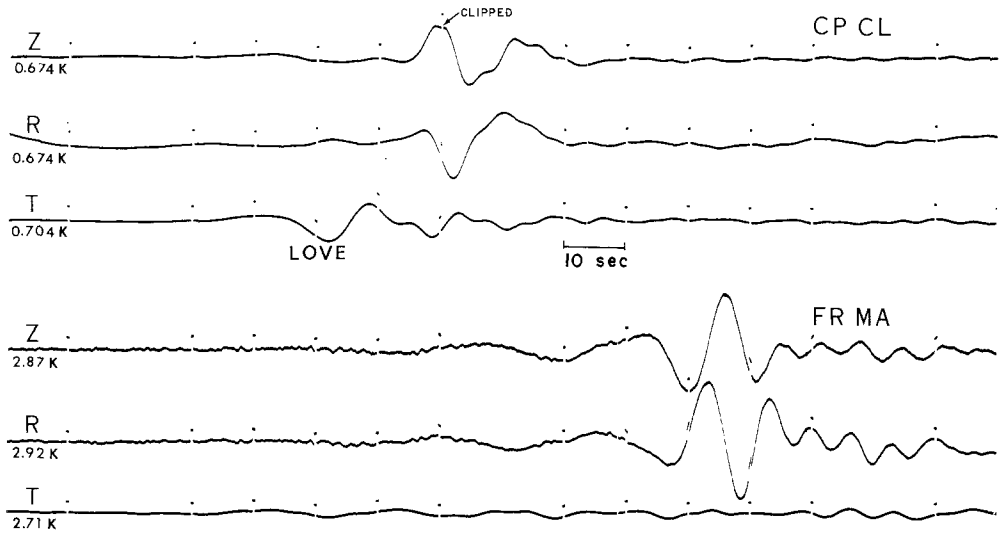

FIG. 1. Long-period seismograms of the BILBY explosion (origin time: 17:00:00 GMT, depth: 700 m, medium: tuff, equivalent magnitude: m_b = 5.8) at two LRSM stations: CP-CL (Campo, California, Δ = 482 km) and FR-MA (Forsyth, Montana, Δ = 1282 km). Time marks are 10 sec apart. Z indicates vertical, R and T the horizontal components, respectively. Numbers are relative magnification of each component. Note the absence of Love waves at FR-MA.

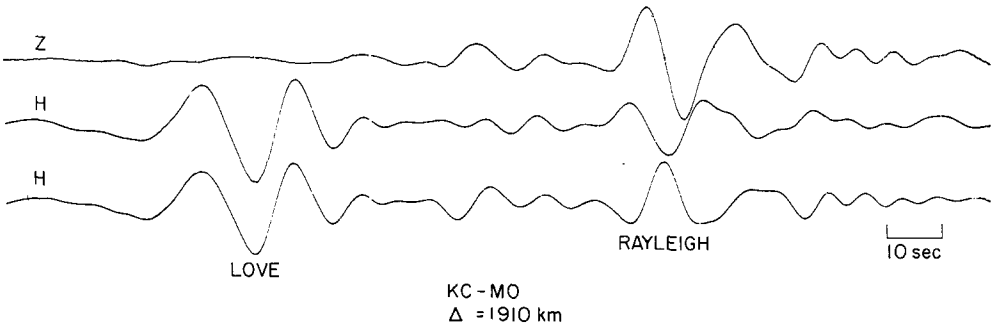

FIG. 2. Love and Rayleigh waves from the explosion GREELEY, recorded at Kansas City, Missouri. Z, H are vertical and horizontal components, respectively.

Here, we illustrate the method with data from the nuclear explosion BILBY detonated at the Nevada Test Site on September 13, 1963 at 17:00:00 GMT.

RADIATION OF SEISMIC WAVES FROM THE BILBY EXPLOSION

BILBY generated Rayleigh and Love waves which were well-recorded at a number of LRSM stations. The station distribution is shown in Figure 3. The Love waves could be identified easily since the long-period horizontal instruments were generally oriented in radial and transverse directions relative to the source. Furthermore, for a continental path, Love waves have higher group velocities than Rayleigh waves in the period range of interest.

Radiation pattern of Rayleigh waves. Under ideal conditions, the radiation pattern can be obtained by correcting the observed amplitudes for instrument response, geometric spreading, and attenuation effects. In practice, however, the geological conditions are complicated and the absolute amplitude method is not very effective (Toksöz and Clermont, 1967). Thus, a method of normalization must be considered. The source and the propagation factors cannot be isolated from each other. Therefore, we must consider methods in which one of the variables is held constant while the effect of the other is investigated. We used two methods for the study of relative amplitudes to determine the radiation pattern from BILBY. In the first, we normalize the amplitudes of the Rayleigh waves generated by the explosion (equivalent magnitude $m_b = 5.8$) to those of the collapse event ($m_b = 4.5$) that followed at 17:31:20.5 GMT. In the second, we used the ratio of the Love- and Rayleigh-wave amplitudes to obtain a source function.

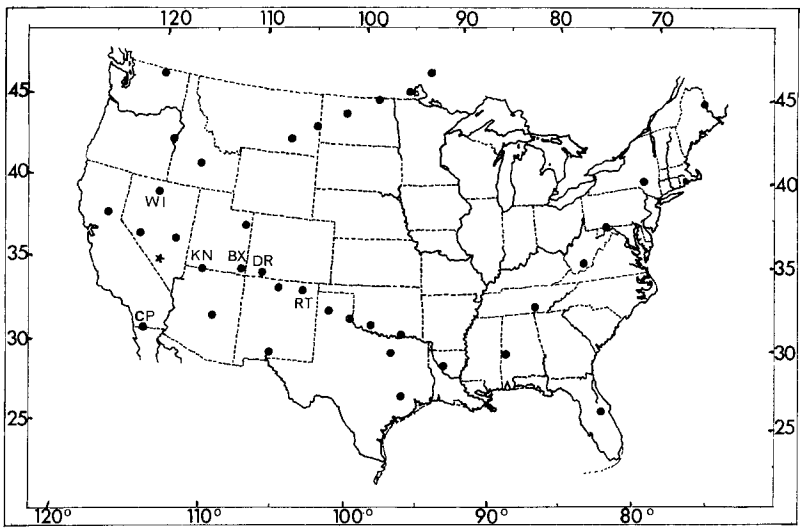

FIG. 3. Distribution of LRSM stations which recorded waves from BILBY in North America. "*Star*" indicates shot location.

The collapse of the cavity (formed by the explosion) seems to provide an excellent reference for normalization. When the amplitude ratios of the explosion- and collapse-generated waves are taken, the propagation and instrument effects completely cancel out, and the ratio directly reflects the source effects. In previous studies, it was found that the radiation pattern from the postexplosion collapse was, in general, more symmetric than the pattern from the explosion. The azimuthally uniform amplitudes as well as the absence of prominent Love waves were evidence of this radial symmetry (Toksöz, 1967). If we assume that the BILBY collapse had a radially uniform radiation pattern, then the explosion to collapse ratio would indicate whether the explosion was a symmetric source.

The ratios of peak amplitudes of the Rayleigh waves are shown in Figure 4 as a function of azimuth. The peak amplitudes were read directly from the long-period records of the LRSM stations and correspond to Rayleigh waves in the period range of 16 to 20 sec. In a few instances, the spectral ratios were computed, and these, on the average, showed a similar radiation pattern as the peak amplitudes.

The azimuthal coverage in Figure 4 is far from being complete, but in the north and northeast directions, where there is a sufficient number of observations, the deviation

from a uniform ratio is clear. If we assume that the radial nonuniformity of the radiation pattern from the explosion was due to some form of tectonic complication (such as the relaxation of the medium due to the cavity or induced rupture), we can include this effect by superimposing a multipolar term on the explosive source. Both seismic model experiments and theoretical studies indicate that at large distances from the source, a double-couple type source function is a good representation for tectonic strain release (Honda, 1962; Burridge and Knopoff, 1964; Archambeau, 1968). Then, the displacements observed at a distant station can be written as the vectorial sums of those due to an explosive source and to a double couple.

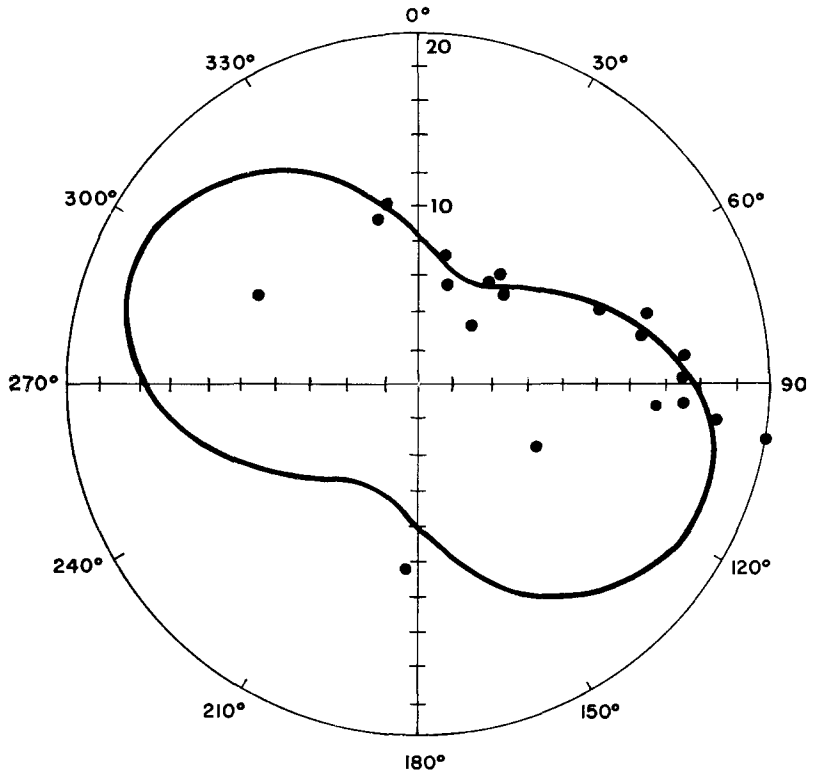

FIG. 4. The radiation pattern of normalized Rayleigh waves for BILBY. The *points* are the ratio of the amplitudes of explosion-generated to collapse-generated Rayleigh waves. The *curve* is the theoretical radiation pattern for a composite source consisting of an explosion and an orthogonal double-couple.

Using the notation of Toksöz, *et al.* (1965), we can write the far-field expressions for the Rayleigh-wave ground displacements from a near-surface explosive source.

$$W_e(\omega) = \frac{c_1}{(2\pi r)^{1/2}} k_R^{1/2} \left(\frac{\dot{U}_0^*}{\dot{W}_0}\right) A_R(\omega) T(\omega) \exp(-\gamma_R r) \exp[i(\omega t - k_R r - \phi_t + 3\pi/4)]$$

$$U_e(\omega) = \frac{c_1}{(2\pi r)^{1/2}} k_R^{1/2} \left(\frac{\dot{U}_0^*}{\dot{W}_0}\right)^2 A_R(\omega) T(\omega) \exp(-\gamma_R r) \exp[i(\omega t - k_R r - \phi_t - 3\pi/4)]$$

$$V_e(\omega) = 0. \qquad (1)$$

Where c_1 is a constant proportional to source strength, $W_e(\omega)$, $U_e(\omega)$, $V_e(\omega)$ are the vertical, radial, and tangential components of the displacement, k_R is the wave number, r is the radial distance, γ_R is the Rayleigh-wave attenuation coefficient. A_R is the medium response for Rayleigh waves due to a vertical force, $\dot{U}_0$ and $\dot{W}_0$ are the components of particle velocity at the surface. $T(\omega)$ and $\phi_t(\omega)$ are the amplitude and the phase spectra of the source-time function. The displacements due to an orthogonal, horizontal double-couple source are (Ben-Menahem and Harkrider, 1964; Toksöz *et al.*, 1965)

$$W_{dc}(\omega) = \frac{c_2}{(2\pi r)^{1/2}} k_R^{1/2} \left(\frac{\dot{U}_0^*}{\dot{W}_0}\right) A_R(\omega) T'(\omega) \sin 2\theta \exp(-\gamma_R r) \cdot \exp[i(\omega t - k_R r - \phi_t' + 3\pi/4)]$$

$$U_{dc}(\omega) = \frac{c_2}{(2\pi r)^{1/2}} k_R^{1/2} \left(\frac{\dot{U}_0^*}{\dot{W}_0}\right) A_R(\omega) T'(\omega) \sin 2\theta \exp(-\gamma_R r) \cdot \exp[i(\omega t - k_R r - \phi_t' - 3\pi/4)]$$

$$V_{dc}(\omega) = \frac{c_2}{(2\pi r)^{1/2}} k_L^{1/2} A_L(\omega) T'(\omega) \cos 2\theta(-\gamma_L r) \cdot \exp[i(\omega t - k_L r - \phi_t' - 3\pi/4)]. \quad (2)$$

The subscripts R and L refer to Rayleigh and Love waves, respectively. c_2 is the source constant, and the angle θ is measured counterclockwise from the principal plane (i.e., fault plane) of the double couple.

The far-field displacements of Rayleigh and Love waves from a composite source consisting of an explosion and horizontal double couple can be written from (1) and (2).

$$U_{Rz} = W_e(\omega) + W_{dc}(\omega) = W_e(\omega)\left\{1 + F\frac{T'(\omega)}{T(\omega)} \sin 2\theta \exp[i(\delta\phi_t)]\right\}$$

$$U_L = V_{dc}(\omega). \quad (3)$$

F is the relative strength of the double couple, $\delta\phi_t = \phi_t' - \phi_t$ is the phase difference of two time functions. The term with the factor sin 2θ gives the azimuthal dependence of the Rayleigh-wave radiation.

If we assume that the source-time functions are approximately the same for an explosion and the multipolar source in the period range of interest (i.e., $T = T'$), equation (3) becomes

$$U_{Rz} = W_e(1 + F \sin 2\theta)$$

$$U_L = V_{dc}. \quad (4)$$

The motion from the collapse of the cavity can be represented by

$$(U_{Rz})_{\text{collapse}} = C_3 W_e \exp(i\phi_c) \quad (5)$$

where C_3 is the relative amplitude and ϕ_c is the phase of time function relative to the explosion. From previous studies, it was found that at long periods ($T \approx 20$ sec), explosion and collapse pairs had similar spectra except for a phase term $\phi_c \approx \pi$ (Brune and Pomeroy, 1963; Smith, 1963; Toksöz *et al.*, 1964). With the above formulations and assumptions, the theoretical Rayleigh-wave displacement ratios for a given explosion-collapse pair can be written as

$$\frac{(U_R)_{\text{explosion}}}{(U_R)_{\text{collapse}}} = C'[1 + F \sin 2\theta]. \tag{6}$$

In Figure 4 the theoretical curve is computed using (6). Choosing C', F, and the orientation of the double couple to fit the data best, we find $C' = 12$, $F = 0.47$, and the reference direction for the double-couple principal plane (i.e., "fault plane") $\theta = 340°$. With these data, the fit is good. The above figures mean that the explosion-generated

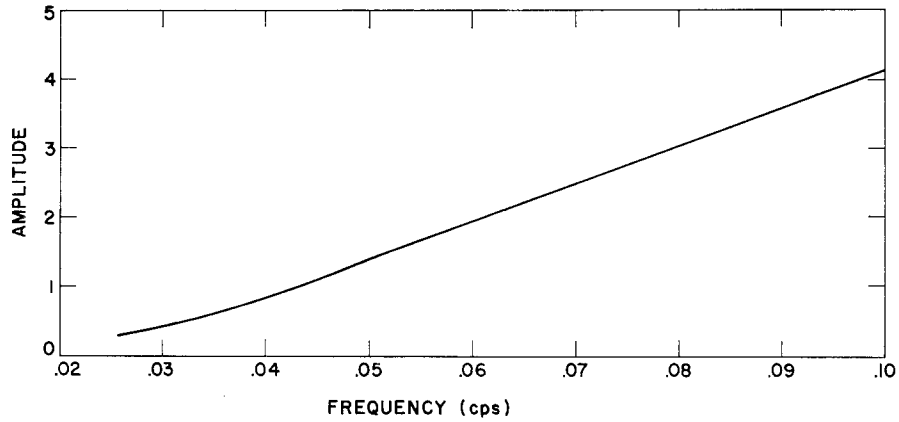

FIG. 5. Rayleigh-wave amplitude response of the layered medium to an explosive source near the surface, with impulsive time function.

surface waves were 12 times larger than those of the collapse, and that the relative strength of the double-couple force was 0.47 times that of the explosion.

Amplitude ratios of the Love and Rayleigh waves. The Love waves generated by the explosions can also be used to determine the nature of the source mechanism. According to our formulation, the Love waves will be generated by the tectonic component of the source. In determining the radiation pattern, we will again use a normalization scheme to minimize the effects of propagation paths and recorder magnifications. Since we do not have a pure Love-wave source that can be used as a reference, we will normalize to Rayleigh waves.

The ratio of the Love-wave amplitude to the Z component of the Rayleigh waves generated by the explosion can be written using equations (1), (2), (3), and (4).

$$\frac{|U_L|}{|U_{Rz}|} = \frac{Fk_L^{1/2} A_L \cos 2\theta}{(1 + F \sin 2\theta) k_R^{1/2} A_R (\dot{U}_0^*/\dot{W}_0)} \exp[-r(\gamma_L - \gamma_R)]. \tag{7}$$

In writing (7), it was assumed that the source-time functions $T(\omega)$ and $T'(\omega)$ were the same for both the explosion and the double-couple component. Furthermore, as in the previous section, it is assumed that the tectonic contribution can be represented as a

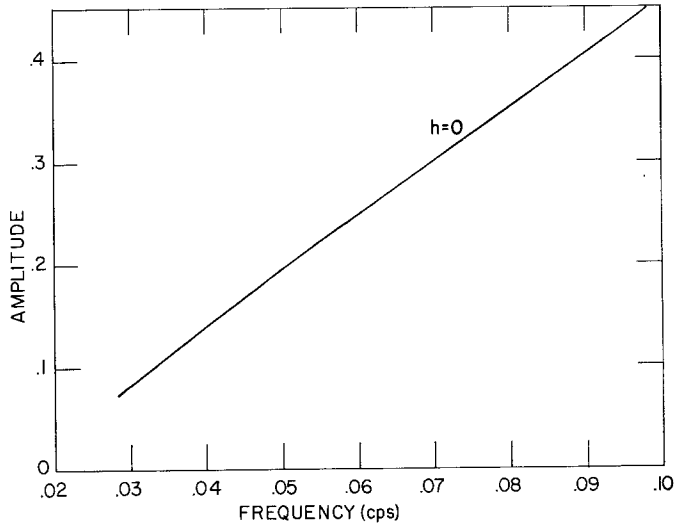

FIG. 6. Love-wave amplitude response of the medium to a double-couple source near the surface.

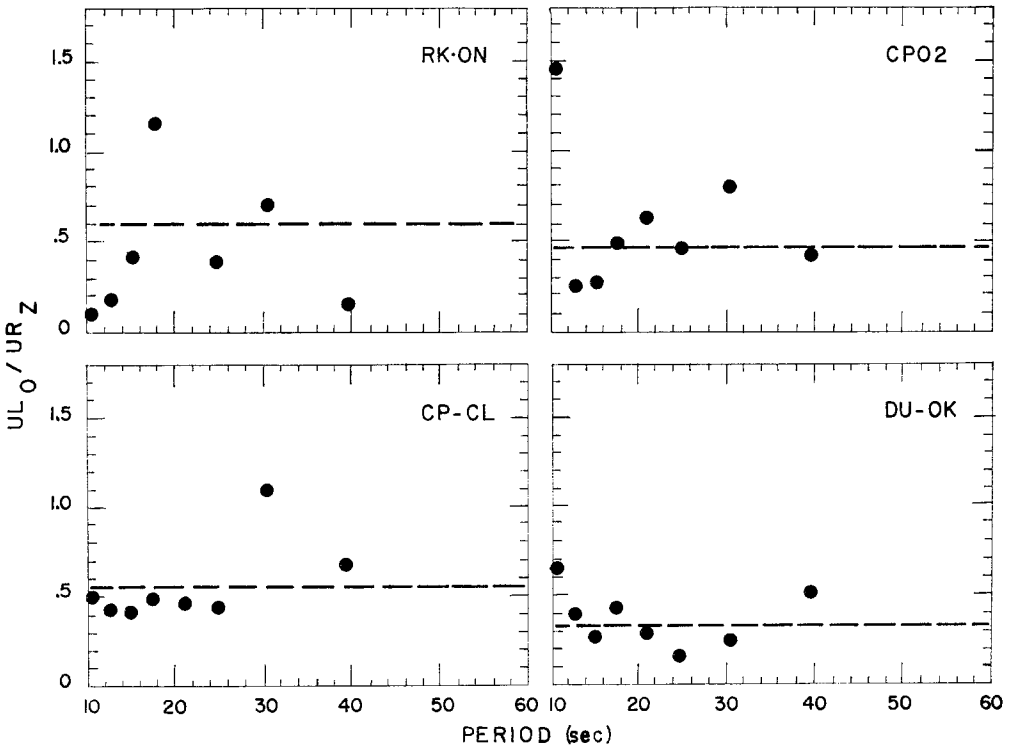

FIG. 7. Love-wave to Rayleigh-wave vertical component Fourier amplitude spectral ratio at four stations. *Dashed lines* are the ratios of peak amplitudes measured in time domain.

double couple. Thus the Love waves are those generated by a double couple, and the Rayleigh waves are the vectorial sum of those due to the explosion and due to the double couple.

In using (7) we must compute k_L, A_L, k_R, A_R, $(\dot{U}_0^*/\dot{W}_0)$, γ_L, γ_R. These quantities

are functions of the frequency for a given earth structure. Fortunately, $k_L^{1/2}A_L/k_R^{1/2}A_R$ is a monotonic and slowly varying function of frequency in the spectral range of our interest. Thus, the effect of the structure is minimized by the normalization process, and an imprecise knowledge of structure does not limit the applicability of the method. We took one average structure for the Western United States given by Alexander (1963) and computed the amplitude response for the Rayleigh (A_R) and the Love (A_L)

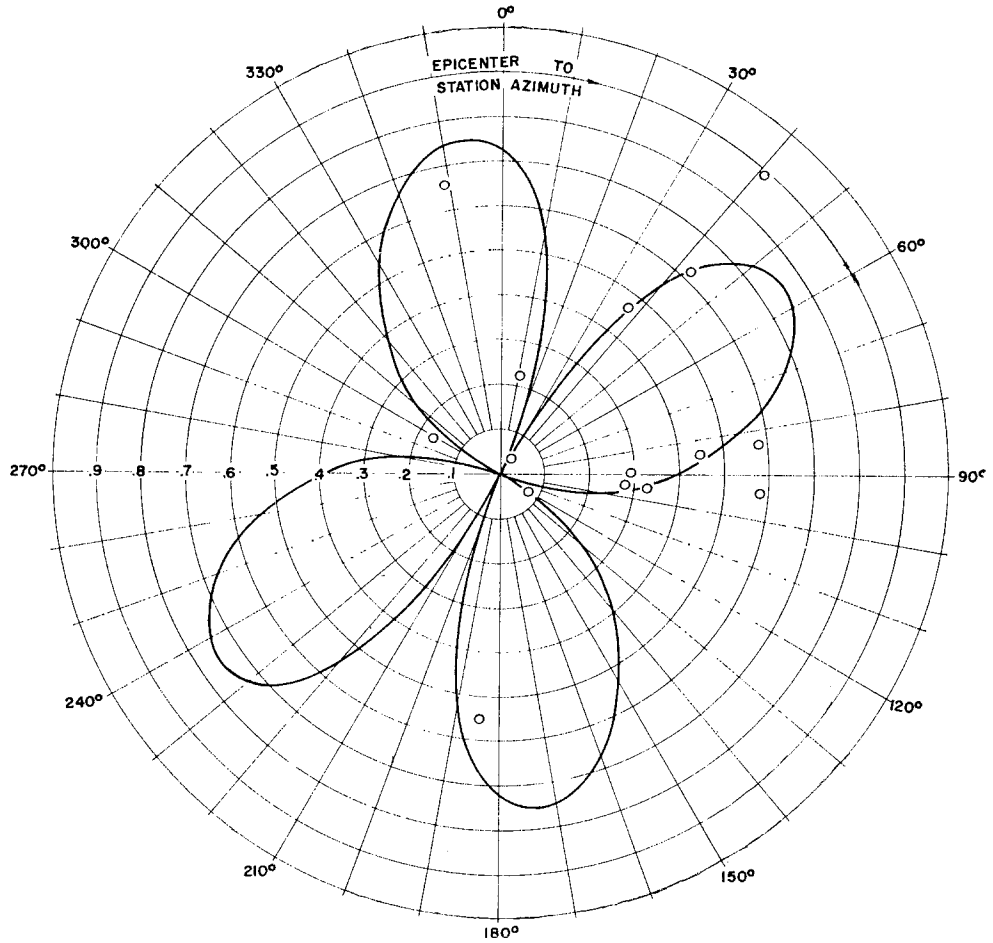

FIG. 8. Amplitude ratios of the explosion-generated Love and Rayleigh waves (U_L/U_{Rz}) as a function of azimuth. The *theoretical curve* is for the composite source described in Figure 4.

waves. The method and programs of Harkrider (1964) were used in these computations. The results are shown in Figures 5 and 6.

In computing the Love to Rayleigh amplitude ratios from the long-period recordings on the LRSM stations, we used the peak amplitudes. In cases where spectra were computed, they peaked at about $T = 18$ sec. Spectral ratios are shown in Figure 7 for four stations, together with the ratio of peak amplitudes. On the average, the agreement is good enough to justify the use of peak amplitudes, with the understanding that the results are valid only in the $T = 15$- to 20-sec period range. At longer periods, U_L/U_{Rz} ratios generally tend to increase as seen for stations CP-CL and CP02 in Figure 7.

All the available U_L/U_{Rz} data from BILBY are shown in Figure 8, as well as the

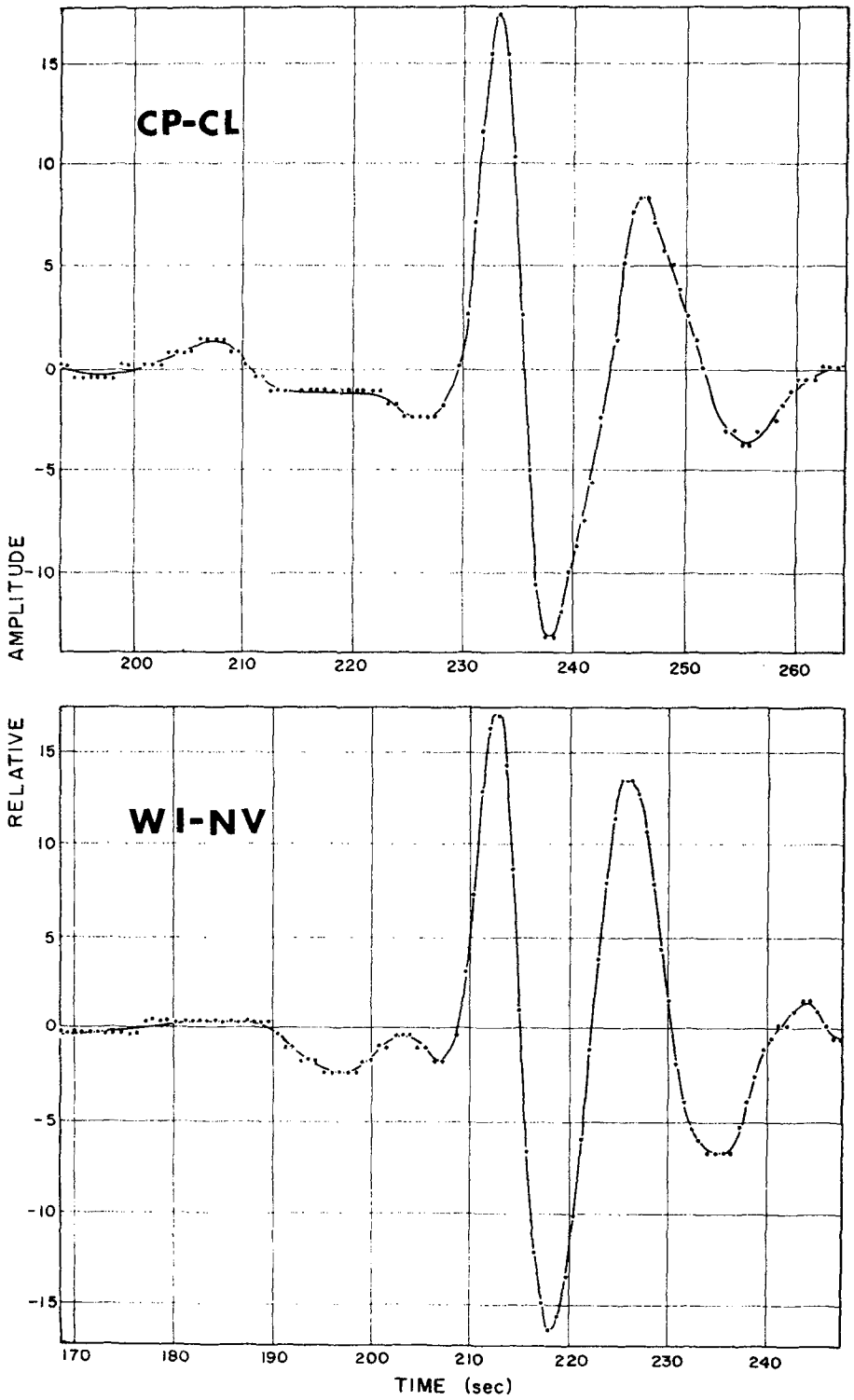

FIG. 9. Rayleigh-wave pulses at two stations plotted from digitized data.

theoretical curve based on equation (7). The reference plane for double-couple orientation (plane of $\theta_0 = 340°$) and the relative strength $F = 0.47$ are the same values that were determined from the explosion-to-collapse Rayleigh-wave ratios. The agreement between the observed data and the theoretical curve can be considered good.

The consistency of one single source model for both the Rayleigh- and the Love-wave radiation patterns is encouraging. Although this is not a definite proof, it gives support to our method of synthesizing the source and to our assumptions.

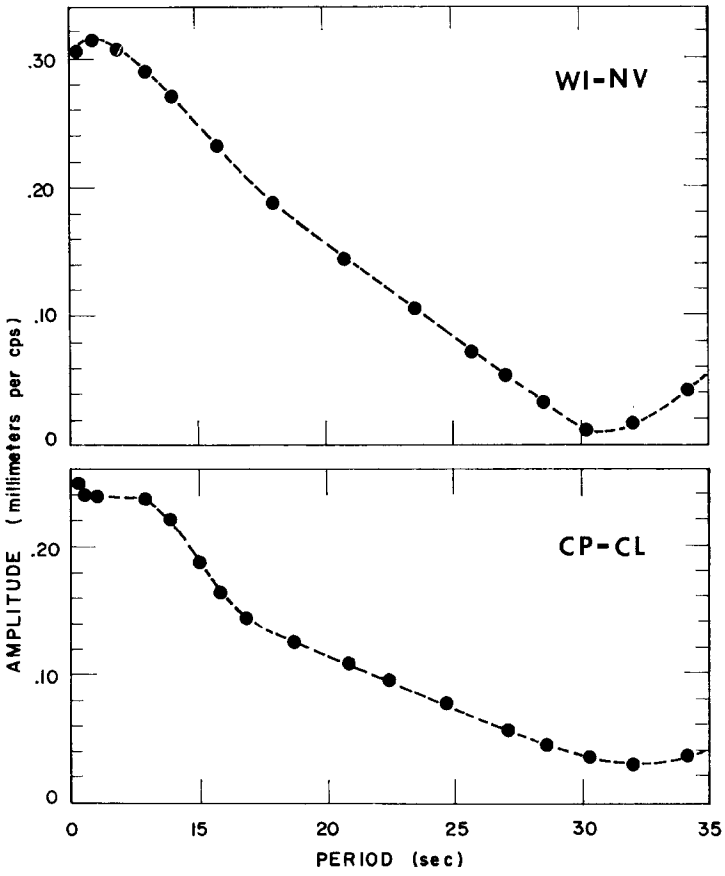

FIG. 10. Ground displacement spectra (corrected for instrument response).

SOURCE-TIME FUNCTION OF BILBY

The source-time function of the explosion can be determined from the recordings of the motion at distant stations by correcting for the instrument response and the response of the propagation medium. In this study, we will use an average structure and use only the amplitude response, since the accuracy of phase spectra depends very strongly on exact knowledge of the structure.

The Rayleigh waves recorded at three stations are first corrected for the instrument response to obtain the true ground displacement. These stations are Kanab, Utah (KN-UT), Campo, California (CP-CL), and Winnemucca, Nevada (WI-NV). They represent excellent azimuthal coverage at fairly close distances (see Figure 3). Rayleigh-wave pulses, filtered in the passband $T = 6$ to 40 sec, are shown in Figure 9 for two

stations. Ground displacement spectra (Figure 10) are obtained by correcting the Fourier amplitude spectrum for the instrument response (for instrument response see the report: "Long Range Seismic Measurements, BILBY," prepared for AFTAC by the Data Analysis and Technique Development Center, Teledyne, Inc., *DATDC*

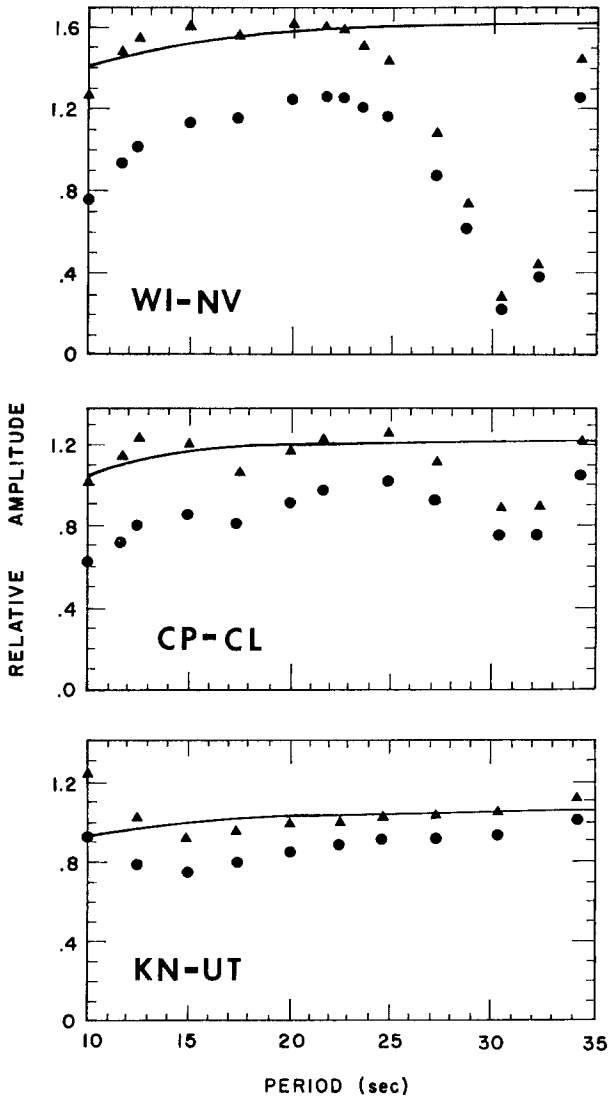

FIG. 11. Amplitude spectra of source-time function after correction for propagation effects. *Circles* indicate data uncorrected for attenuation; *triangles* indicate the data corrected taking $Q = 100$. Lines are theoretical curves for source-time function shown in Figure 12.

Report No. 87, September 13, 1963). These spectra represent the product of the source amplitude spectrum and the response of the layered medium (i.e., propagation path) to Rayleigh waves. The medium response includes the effects of attenuation and the source depth.

To determine the source function, we must correct the ground displacement for the propagation factor. This was done using the impulse response of the medium (Figure

5) as given by equation (1). The effect of attenuation was removed using $\gamma_R = \pi f/UQ$ where U is the group velocity and Q was assumed to be 100, independent of frequency. The corrected spectra are shown in Figure 11. This presumably represents the spectrum of the source-pressure function.

The interpretation of amplitude spectra in terms of a time function requires incorporating either phase data or some other constraint. We will follow Toksöz, *et al.* (1964) and assume that the pressure pulse has the form $p(t) = p_0 t \exp(-\eta t)$. The whole problem now consists of determining the parameter η from the spectra. A value of $\eta = 1.5$ seems to agree well with the observations as shown in Figure 11. Discrepancies at periods longer than $T = 30$ sec are attributed to the effects of lateral heterogeneities and low signal to noise ratio. Scattering effects and possible variation of Q versus frequency may contribute to the deviations. The time function is given in Figure 12.

We must note here that the $p(t)$ we determined represents the stress-wave form not

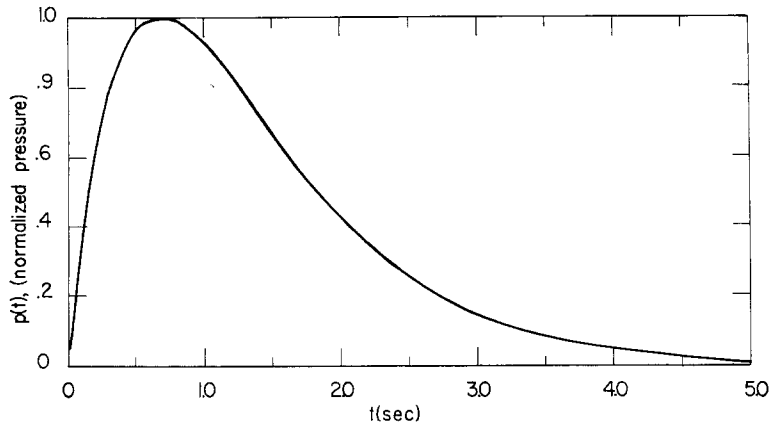

FIG. 12. The Rayleigh-wave source-time function for BILBY at the boundary of the seismic zone where strains are infinitesimal.

at the source but at some distance from the point of detonation. Since we used a linear theory based on infinitesimal strains to correct for propagation and attenuation effects, our corrections are valid only to the boundary of the region where these conditions are met. This may be at a distance of several kilometers from the source point. We must clarify one other aspect of Figure 12: the pressure pulse was based on data in the period range of 10 to 35 sec, so we could not see any of the fine features of the pulse that would be observable primarily in the high-frequency components. Neither could we see a small residual permanent displacement or strain. Even with these limitations, the shape of the time function shown in Figure 12 is similar to (although somewhat broader than) those of close-in measurements (Wistor, *et al.*, 1963; Perrett, 1968). The source-time function varies since it is dependent on the yield of the explosion, the medium, and shot depth. In general, larger explosions have broader pulses (smaller η values). Other investigators have also proposed a step-function for the source model on the basis of surface-wave data (Tsai and Aki, 1971). However, the available close-in acceleration measurements (Perrett, 1968) and near-field strain data (Smith, *et al.*, 1969) indicate larger stresses at the beginning of the pulse than toward the tail. These emphasize the need for spectral data near the source over a broad period range for future detailed source studies.

To examine the source function of the Love waves generated by BILBY, we chose four stations where Love waves are well separated from Rayleigh-wave interference and corrected the spectra for the instrument response and the response of the layered medium for an orthogonal double-couple source. The resultant spectra of the source-time function are shown in Figure 13, and their shapes are consistent for all four stations.

From the comparison of Figures 11 and 13, it is obvious that the source-time func-

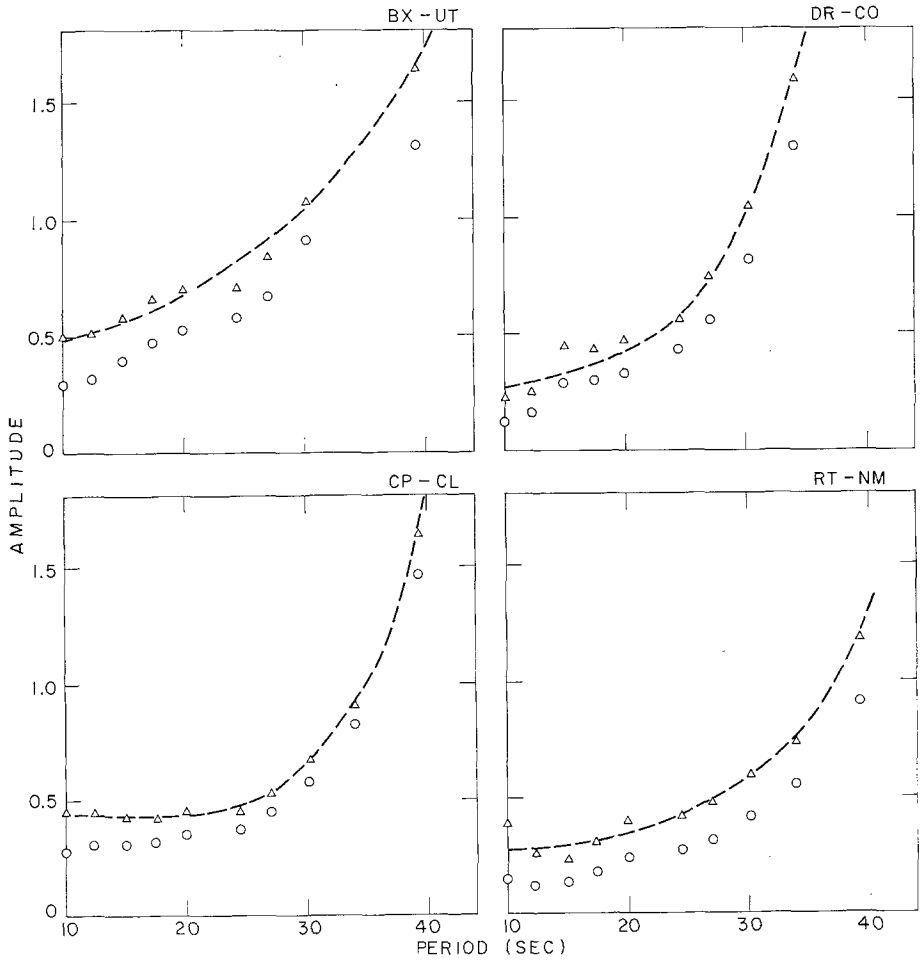

FIG. 13. Amplitude spectra of source-time function for Love waves after correction for propagation effects. *Circles* are uncorrected; *triangles* are corrected for attenuation taking $Q = 100$.

tion of the explosion-generated Rayleigh waves and that of the Love waves is quite different. The Love waves seem to be richer in low-frequency components. From the available amplitude data in a relatively narrow frequency band, we cannot determine the *time* function of Love waves. It appears to be between a step function and a ramp, if we assume a point source near the surface, a value of $Q = 100$, and if we ignore the effects of source volume. With these limitations, a step function with a rise time on the order of a few seconds may be an acceptable approximation for Love waves.

The source spectra of the Rayleigh and Love waves generated by explosions are important because they contain information about the mechanism of the Love-wave generation. The differences demonstrated above are significant. They indicate that an

explosion may trigger the Love-wave radiation, but it probably does not control its time history. The Love-wave source spectra are closer to those of earthquakes than to the spectra of explosion-generated Rayleigh waves.

Comparison with other Explosions.

In determining the source properties of the BILBY explosion, we followed the same procedures that were used in our earlier studies of the HARDHAT, HAYMAKER, SEDAN and SHOAL explosions, as well as in some later events (Toksöz, *et al.*, 1965; Kehrer, 1969; Toksöz *et al.*, 1971). Here, we will compare the BILBY results with those of other explosions, which are tabulated in Table 1.

The most significant result is that BILBY, like the HAYMAKER and SHOAL explosions, generated Love waves. The source mechanism in all cases can be explained in terms of an ideal radial explosive source superimposed on a tectonic source of double-

TABLE 1

List of Explosions and Relative Strength of Double-Couple Components

Explosion	Date	Region	Medium	Double-Couple Strength (T = 20 sec)	Fault Azimuth (deg)
HARDHAT	2-15-62	Yucca Flat (n. end)	Granite	3.00	330°
SHOAL	12-26-63	Fallon, Nevada	Granite	0.90	346°
CHARTREUSE	5-6-66	Pahute Mesa	Rhyolite	0.94	353°
HALF BEAK	6-30-66	Pahute Mesa	Rhyolite	0.67	345°
			Zeolitized		
BENHAM	12-19-68	Pahute Mesa	Tuff	0.85	345°
CORDUROY	12-3-65	Yucca Flat	Quarzite	0.72	347°
CUP	3-26-65	Yucca Flat	Tuff	0.55	200°
BILBY	9-13-63	Yucca Flat	Tuff	0.47	340°
TAN	6-3-66	Yucca Flat	Tuff	0.39	340°
HAYMAKER	6-27-62	Yucca Flat	Alluvium	0.33	340°
SEDAN	7-6-62	Yucca Flat	Alluvium	0	—
SALMON	10-22-64	Hattiesburg, Miss.	Salt	0	—
GNOME	12-10-61	Carlsbad, New Mexico	Salt	0	—

couple form. The orientation and relative strength of the double couple seem to be controlled by the properties of the medium and the orientation of the tectonic axes in the source region. BILBY (in tuff) and HAYMAKER (in alluvium) were located about 5 km apart. The radiation patterns of Rayleigh waves are almost identical. In both cases, the principal plane of the double-couple is oriented in the direction $\theta = 340°$. Other explosions in the same general area give similar orientation. In the SHOAL explosion, which was fired in a completely different area, the orientation of the double couple was in very good agreement with those of earthquakes in the area (Toksöz *et al.*, 1965). These facts suggest that multipolar contributions to the radiation patterns are controlled by the general tectonic features of the region.

The relative strength of the tectonic (double-couple) contribution to the radiation pattern seems to be controlled by the properties of the medium in which the explosion is detonated. This is demonstrated by the observation that for explosions in salt domes (GNOME and SALMON) and loose alluvium (SEDAN), the source functions did not have multipolar components (i.e., $F = 0$). For HAYMAKER, which was buried deep in alluvium, a value $F = 0.33$ was determined. For BILBY (in tuff) F was 0.47, and for SHOAL, which was fired in granite, F was equal to 0.9. HARDHAT

was another explosion in granite, and it had an F value greater than 1.0. These and ten other explosions recently studied (Toksöz, *et al.*, 1971) indicate an increase of F with increasing rock strength and, hence, strain energy capacity of the medium.

From these examples we cannot determine conclusively whether the multipolar component of the seismic energy radiation is due to release of some of the strain energy accumulated in the medium, due to fracturing or due to earthquake triggering. Our laboratory model experiments, described below, will help to clarify some of these points.

Laboratory Experiments

Laboratory experiments can, in principle, provide a better physical understanding of explosive seismic sources than field observations because the explosive source strength, prestress field, and elastic properties of the medium can be varied in a known way. Two separate laboratory experiments were carried out with explosions in pre-

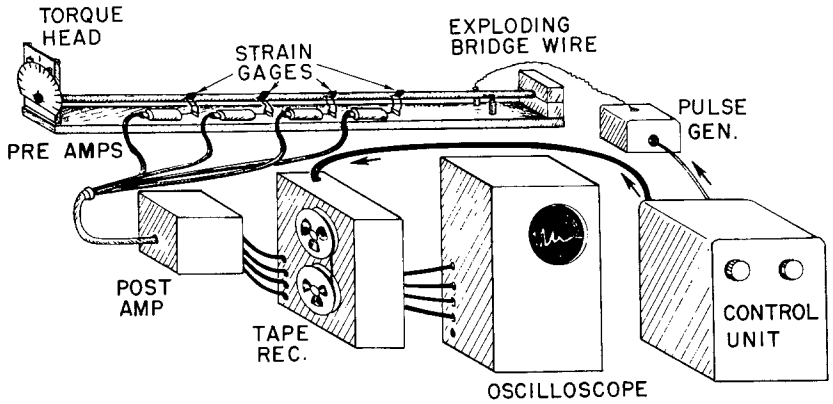

Fig. 14. Laboratory set-up for one-dimensional experiment. Stress waves from an explosive source in a rod under torsion are recorded by strain gauges.

stressed media. The first experiment utilized a rod stressed in torsion, an explosive source, and strain gauges. The second set of experiments was performed with point sources in a prestressed two-dimensional plate model. Photoelastic techniques and high-speed photography were utilized to determine the shot effects in the source region, radiation of stress waves, and the crack formation as a function of medium properties and prestress levels

Stressed Rod Experiment.

A simple one-dimensional laboratory experiment, giving insight into the basic physical mechanisms involved in the production of stress waves from explosive sources in prestressed media, is shown in Figure 14. Plexiglas rods 1.27 cm in diameter, and of varying lengths up to 2 m, were stressed in torsion. A few centimeters from one end, a bridge wire was inserted in a close-fitting diametric hole and exploded with a 100-joule source. This was adequate energy to sever the end of the rod leaving the remainder of the rod free from the torsional restraints holding it. The resulting radiated waves were recorded by strain gauges placed on the rod circumference at various distances from the shot but oriented at 45° to the rod axis. Typically, four gauges were used, one

recording directly onto an oscilloscope, and all four were recording on magnetic tape. The gauges were also read statically before firing the bridge wire source to provide a measure of the prestrain.

Typical oscillogram tracings from four shots at different prestress levels are shown in Figure 15. Two outstanding pulses on the oscillogram are the one-dimensional equivalents of P and S waves. Velocities measured, using gauges at several distances from the source, identify these as the rod wave (P) and torsion wave (S), respectively. The distinctive wave shapes for P and S pulses in Figure 15 indicate that P-wave shape is controlled by the time function of the explosive source. The S-wave is characterized by a step-function input corresponding to the permanent relaxation of the torsional strain in the medium.

A number of oscillograms were obtained at various prestrain levels but with the

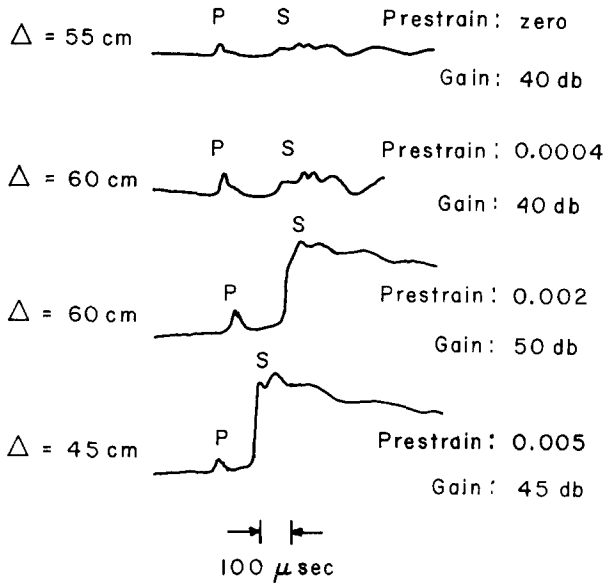

FIG. 15. Strain-gauge seismograms from one-dimensional experiment at different prestress values.

same explosive source. The amplitudes of the P and S waves are plotted as a function of the prestrain level in Figure 16. It is quite apparent that the amplitude of the S-wave, due to strain release, increases linearly with an increase in the prestressing field while the P-wave amplitude remains constant. From the zero intercept times for both P and S waves in time-distance plots, it can be concluded that, at the precision level of this experiment, there was no evidence of a different origin time for P than for S. Furthermore, the observed time function of radiated S-waves (Figure 15) can be characterized as a Heaviside step function, as seen through response of strain gauges. This is consistent with the source-time function observations for the Rayleigh waves and the Love waves from the BILBY explosion, as determined above.

TWO-DIMENSIONAL PHOTOELASTIC EXPERIMENTS

The one-dimensional experiment cannot be used to model the spatial variation of radiation pattern from explosive sources in prestressed media. However, a close simulation of the underground explosions can be achieved by using two-dimensional modeling techniques.

The experimental procedure used in this study involved glass and plexiglas plates stressed in tension or shear. The explosive source was simulated by a small radial shot and the source and radiation fields were observed by dynamic photoelastic techniques. In addition to the above, strain gauge measurements, similar to those of Kim and Kisslinger (1967), were carried out simultaneously. The use of glass as a model material was important because its shock-loading properties are closer to those of rock-forming silicates than are the properties of more ductile, but experimentally more convenient, plastics or metals.

Figure 17 shows in outline the apparatus used in our two-dimensional work. Explosive excitation of the model was provided by a closed loop of mild detonating fuse (MDF). This induced a radial shock source in the plate as the shock wave from the detonation in the MDF entered the plate model simultaneously from both sides. The

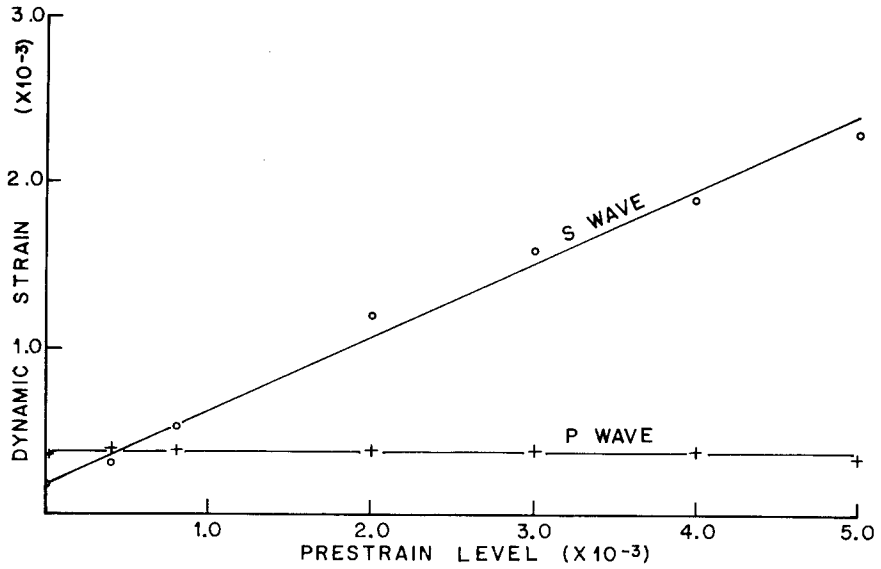

FIG. 16. Amplitudes of P and S waves as a function of prestrain.

model was surrounded by polarizing optics so that the explosion process, cracking, wave generation and propagation could be made visible to the high-speed framing camera by means of the photoelastic effect. Suitably-conditioned, intense paraxial illumination was provided by the Argon bomb, a front-surface mirror, and the Fresnel lens. A much more detailed discussion of the experimental technique, the methods of using dynamic photoelastic observations (isochromatics and isoclinics) to identify seismically interesting features, is given in an earlier paper by Thomson *et al.* (1969), and we will not further elaborate on it here.

In the following section, we will investigate in detail both the propagation of the stress waves from the shot and the characteristics of the cracking phenomena.

Stress-wave propagation in a stressed plate. To understand the fringe patterns shown in Figures 18, 21, and 25, it is necessary to introduce some basic definitions and results of some calculations.

Upon passage through a stressed plate model, monochromatic, circularly polarized light becomes polarized in two orthogonal directions. These are parallel to the principal stress directions in the plane of the plate. Since the light polarized in each direction

experiences a different velocity in traversing the model, an interference effect (isochromatics) is observed when the two components of the incident beams are combined upon passage through the analyzer. The isochromatic fringes are proportional to the difference in the principal stresses $(\sigma_1 - \sigma_2)$ and, hence, the maximum shearing stress. The fringe order n is thus given by

$$n = h\,(\sigma_1 - \sigma_2)/f = \frac{2h}{f}\,|\tau_m| \tag{8}$$

where τ_m is the maximum shear stress, h is the plate thickness, and f is the constant of proportionality which is wavelength dependent. Therefore, if white light is used to illuminate the model, the isochromatic effect is a multicolored interference pattern.

In plane polarized light, an additional set of extinctions, called the isoclinics, are

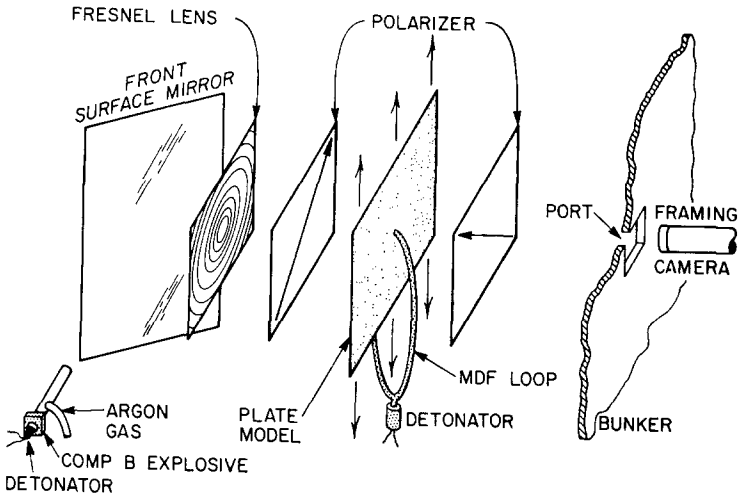

FIG. 17. Experimental set-up for the two-dimensional dynamic photoelastic studies of explosive sources in prestressed media.

seen wherever the principal stress directions are parallel or perpendicular to the pass directions of the polarizer and analyzer. In this experiment, polarizer and analyzer were oriented at 45° and 135°. Thus in the unstressed plate case, shot-generated P waves will have isoclinics in directions $\theta = 45°, 135°, 225°, 315°$. The S-waves from the same source will have isoclinics at $\theta = 0°, 90°, 180°$ and 270°. The isoclinics are used to identify the wave types (P or S) in these experiments.

Examples of isochromatics and isoclinics from a shot in an unstressed plexiglas plate are shown in Figure 18. Note that these patterns are very clear for P-waves, but less clear for S-waves which were much smaller in amplitude. In fact, S-waves can be identified in this case on the basis of the isoclinics. The theoretical isochromatic and isoclinic pattern for a radial transient source in a plate (Thomson, *et al.*, 1969) is given in Figure 19.

To better understand the isochromatics in the immediate vicinity of the shot where wave forms change, we made a theoretical calculation for the cylindrical source in a plate. The analytic formulations of this problem have been given by Kromm (1948). The numerical solution of the integral equation has been discussed by Barker, Toksöz,

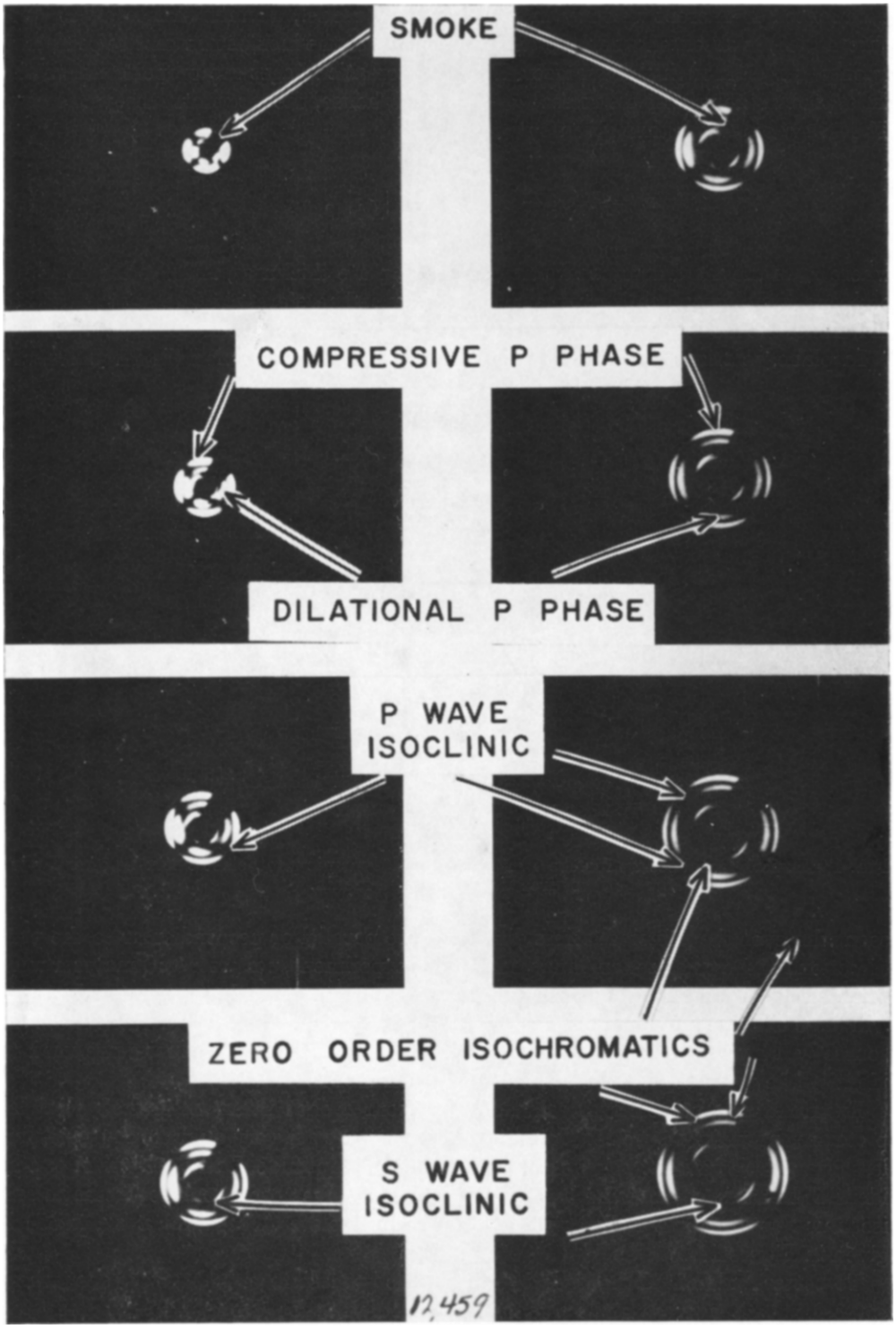

FIG. 18. Isochromatics and isoclinics from a shot in unstressed $\frac{1}{16}$-in thick plexiglas. Interframe time is 4.16 μsec.

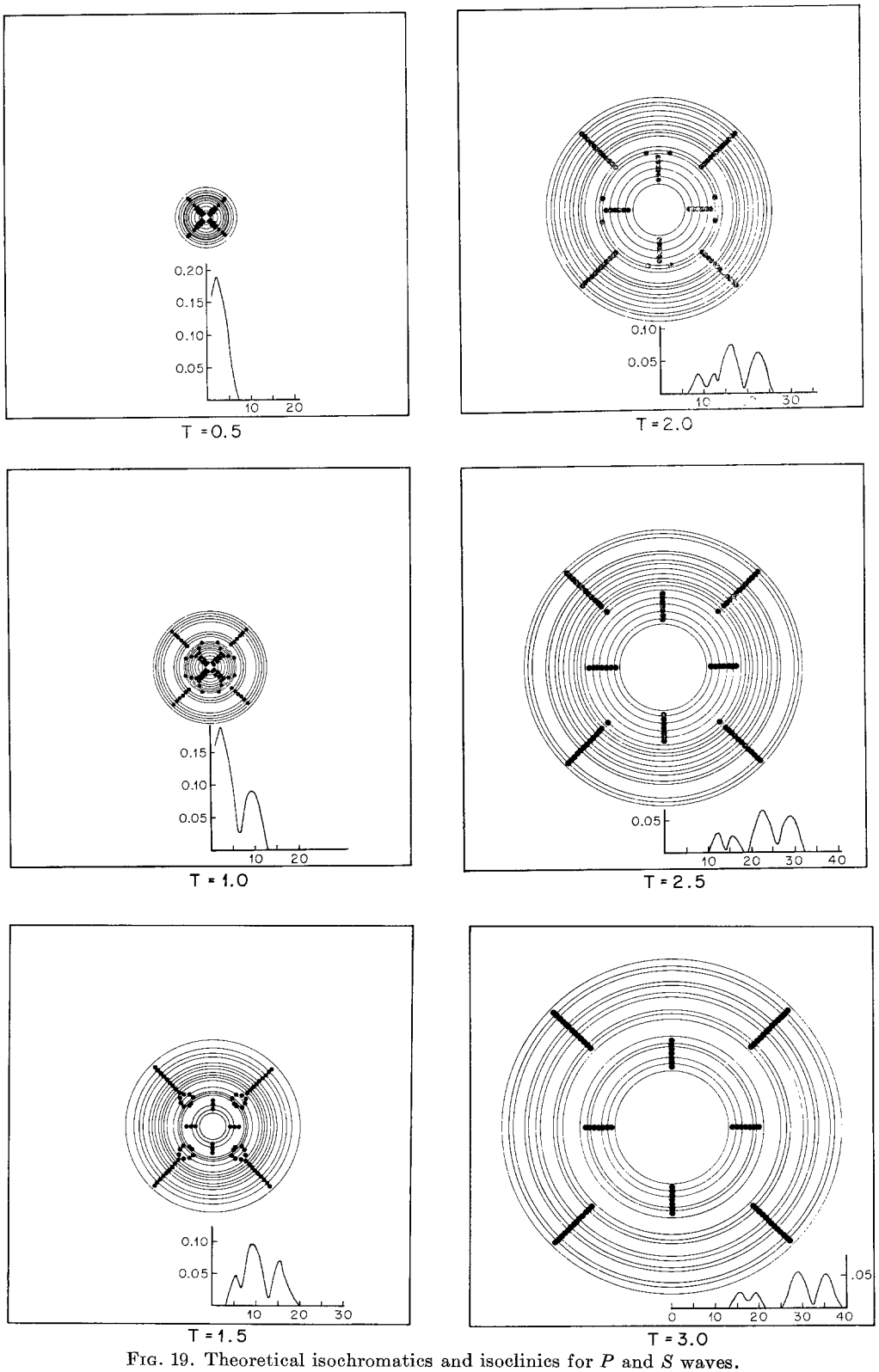

FIG. 19. Theoretical isochromatics and isoclinics for P and S waves.

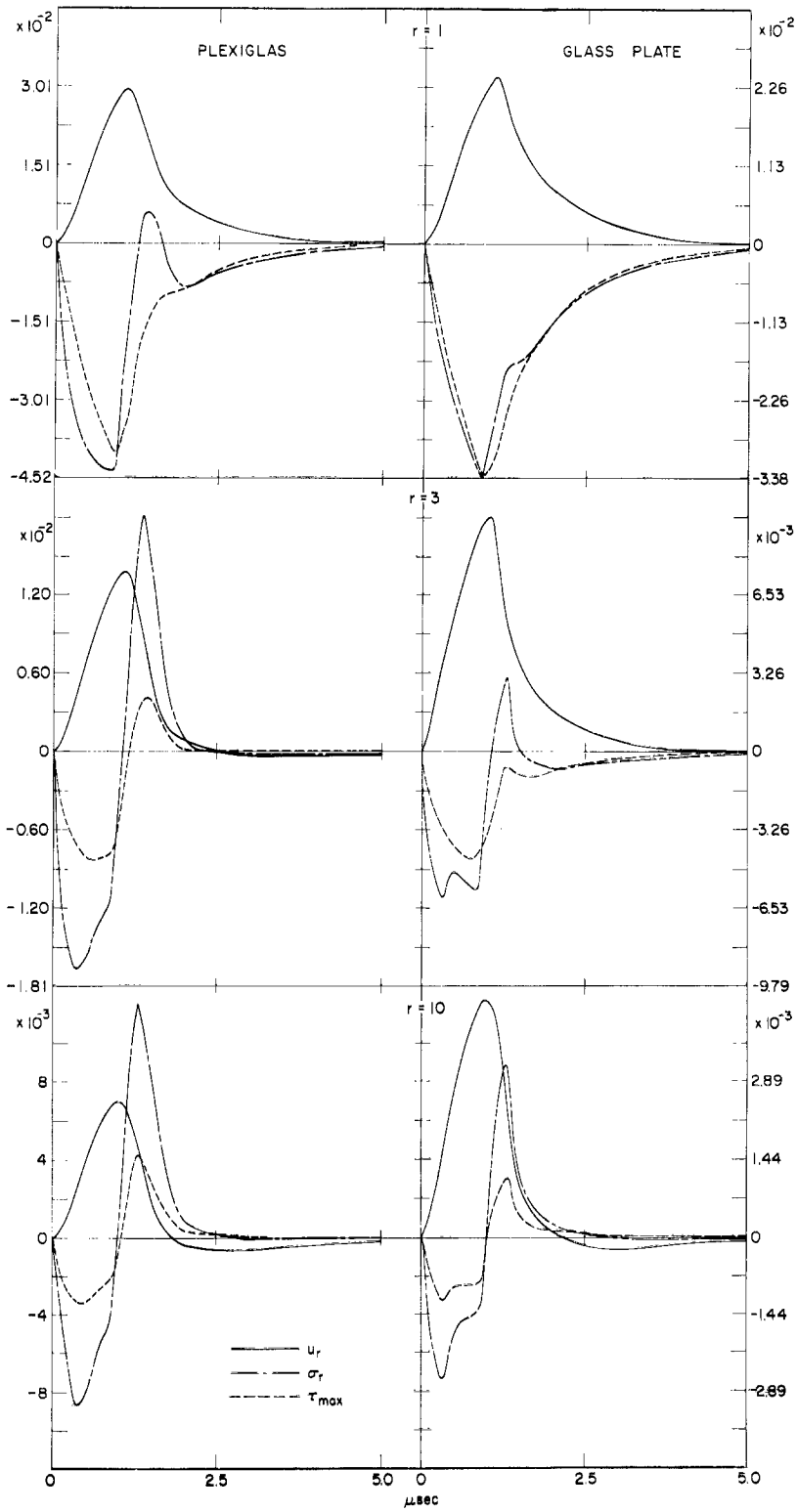

FIG. 20. Theoretical pulse shapes as a function of distance for radial stress and displacement and maximum shear stress, from a cylindrical source in a plate. r is distance in units of source radius (0.185 cm).

and Ward (1969). The results for a particular transient cavity pressure are shown in Figure 20, where the radial stress, displacement, and maximum shear stress have been computed as a function of normalized distance r = distance-to-hole radius from the source for glass and plexiglas. Looking at the maximum shear stress in Figure 20 it is clear that fringes would separate better in the case of plexiglas than in the case of glass as the wave moves farther from the source.

The principal features of Figure 18 were identified by comparing them to the theoretical isochromatics and isoclinics of Figure 19 and to the pulse shapes of Figure 20. Only fractional fringe orders ($n < 1$) are seen in this framing camera sequence. The compressive and dilatational portions of P and the zero-order isochromatic separating them and weak S-waves are all visible in this photograph. The spreading effect on the isoclinics caused by superposition of P and S waves indicated, theoretically, in Figure 19 can be seen, in fact, by close inspection of Figure 18. Color photography was also used in the study to determine absolute stress levels.

The main emphasis of this work is to determine the effect of prestress on the generation and radiation of seismic waves. For this reason, photoelastic experiments with explosive sources were repeated with prestressed plates. The plexiglas and glass plates were stressed in pure tension or pure shear using the stress frame. The shear was generated by applying equal amounts of tension and compression in the y and x directions, respectively. The maximum amount of stress was limited to 167 bars per axis by the strength of model materials.

The static stress field is somewhat complicated by the presence of a small hole (drilled to place the explosive source) in the center of the plate. The radial, σ_r, tangential, σ_θ, and shear, $\tau_{r\theta}$, components of the stress around the hole of radius, a, were computed from Muskhelishvili's solution (Savin, 1966), as in Thomson, *et al.* (1969).

When the explosive source is fired in the prestressed plate, the dynamic stress components are superimposed over the static field described above, producing a complicated isochromatic and isoclinic pattern (Thomson, *et al.*, 1969). These complications make it difficult to extract the dynamic radiation patterns from the framing camera photographs, and, therefore, strain gauge observations were used for this purpose. The radiation pattern of seismic waves from an explosive source in a glass plate under tensile stress is shown in Figure 21. In this figure, in addition to a complicated S-wave radiation pattern, we also see the development and growth of cracking and radiation from crack tips. These experiments were repeated both with plexiglas and glass plates under shear prestress conditions. The radiation patterns were similar to the above cases. In the case of prestressed plates, the shear waves were more abundant than in the unstressed plate experiments.

Strain gauge measurements of P- and S-wave radiation patterns. A set of four BLH foil strain gauges were used to determine the azimuthal variations of P- and S-wave radiation patterns under different prestress conditions. Gauge outputs were recorded on oscilloscopes writing in the single-sweep mode. Each gauge had an active area of 8×10 mm, and this limited its response to periods greater than 4 μsec. In most of the experiments, strain gauges were oriented at 45° to the radial direction and placed at 5 azimuths, at $\theta = 0$, 30, 60, and 90°, at a distance of 16 cm from the source. Since the presence of symmetry was shown from framing camera pictures, instrumenting only one quadrant with strain gauges was sufficient for determining the radiation pattern.

The strain gauge experiments were carried out with shots in both unstressed and stressed plates. In the case of unstressed plates, no significant S waves were detected above the noise level. In the case of prestressed plexiglass and glass plates, however,

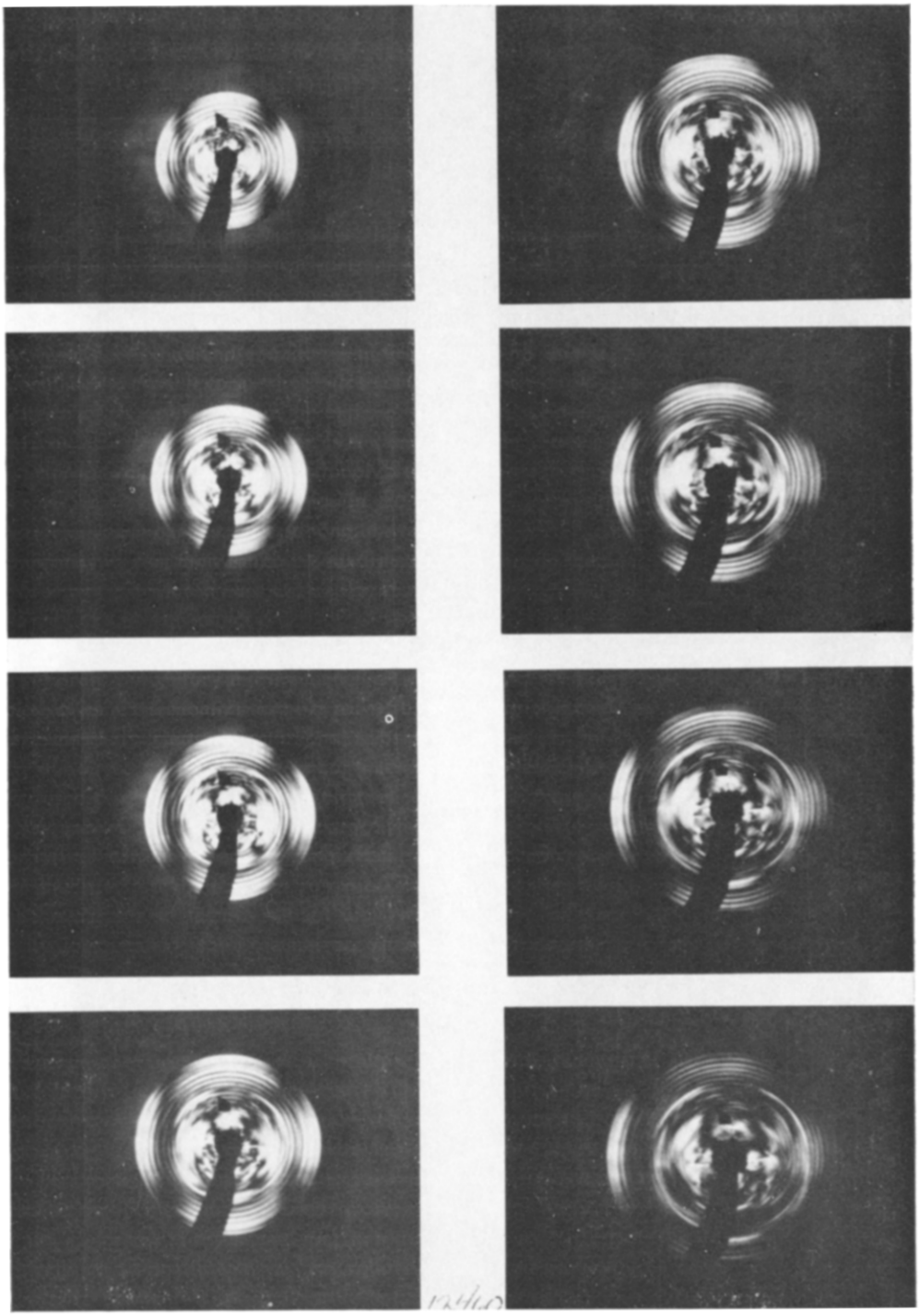

FIG. 21. Isochromatics and isoclinics from a shot in a $\frac{1}{8}$-in thick glass plate stressed under tension (45 bars). Interframe time 2.08 μsec. Note the growth of cracking.

well-defined S waves were recorded. The radiation patterns of P and S waves for plexiglas and glass plates, stressed under tension to 163 bars and 114 bars, respectively, are shown in Figure 22.

Utilizing the local plane-wave formulation, strain energy can be estimated from the observed compressional and shear-wave strains radiated.

$$W = \sum_{i=1}^{3} p_i \epsilon_i \tag{9}$$

where W = energy density and p_i and ϵ_i are principal stresses and strains, respectively. For compressional waves, the strain measured with a gauge oriented at 45° to the radial direction (ϵ) is related as $\epsilon_1 = 2\epsilon$ and for shear waves $\epsilon = \epsilon_1 = -\epsilon_2$. Thus the compressional and shear-wave strain energy density fluxes, W_p and W_s, can be ex-

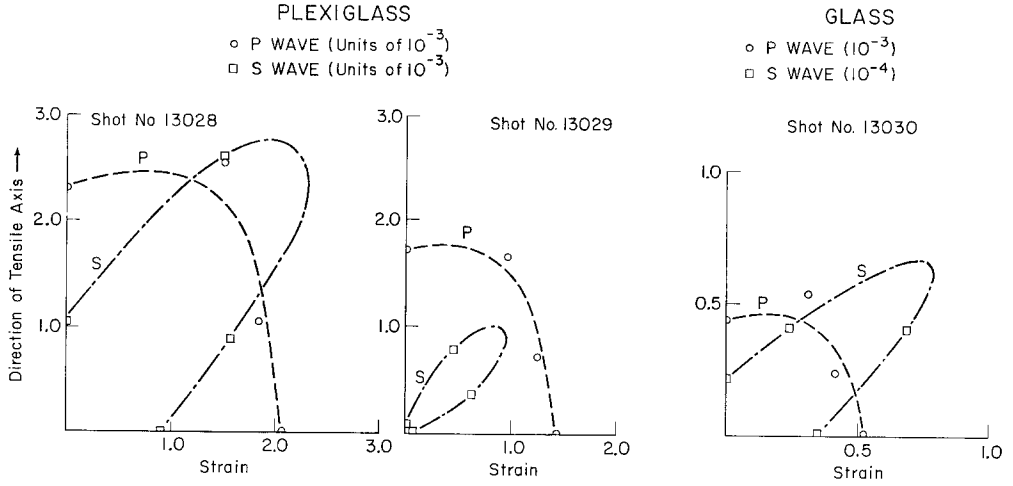

FIG. 22. Dynamic radiation patterns of P and S waves from explosive sources in prestressed plexiglas and glass plates under tension, as measured by strain gauges.

pressed as

$$W_p = V_p \frac{8\nu(\lambda + \mu)}{\lambda + 2\mu} \epsilon^2 = M\epsilon^2 V_p$$

$$W_s = 2\mu\epsilon^2 V_s \tag{10}$$

where V_p and V_s are plate and shear velocities, respectively. For plexiglas and glass used in this experiment, $M = 0.95 \times 10^{11}$ and 13.2×10^{11} dynes/cm^2, respectively. The corresponding rigidities for plexiglas and glass are $\mu = 0.143 \times 10^{11}$ and 2.5×10^{11} dynes/cm^2.

From the radiation patterns of Figure 22, it is clear that the S-wave radiation can be explained by either a dipole or double-couple type source having approximately a sin 2θ azimuthal dependence. The P-wave radiation is less clear since the contribution from the explosion as well as radiation due to prestress are superimposed. It is apparent that the radiation pattern for P would be approximated by a function of θ of the form $(A + B \cos^2\theta)$ where A and B are constants, suggesting again the dipole source with the addition of an isotropic component.

Inspecting the radiation patterns displayed in Figure 22, we are faced with two questions: (1) where does the S-wave energy come from, and (2) what is the reason for the skewness in the P-wave radiation patterns? Let us first consider the energy question. We can compute the P- and S-wave energies by integrating the energy fluxes given in (10) for the duration of the pulse first, and then integrating over the radiation pattern.

At the level of approximation being used here, we can evaluate these integrals by fitting each of the compressional and dilatational half-cycles of strain-wave forms with a half sine wave. Integrating the flux azimuthally, allowing for the radiation pattern, we obtain approximate expressions for the total energy E_P and E_S in P and S waves for each half-cycle of duration t_0

$$E_P \simeq \pi h \rho V_P^3 A_{45}^2 t_0 r$$

$$E_S \simeq \pi h \rho V_S^3 B_{45}^2 t_0 r \tag{11}$$

where h is the model thickness, r is the distance of the strain gauge from the source, and A_{45} and B_{45} are peak strain-gauge readings for the P and S waves, respectively, in the recorded interval under study; the gauges are assumed to be located at the peak of the radiation pattern and oriented at $\pi/4$ to the radius vector from the source. For gauges not located at the peak of the radiation pattern, an additional correction was applied in obtaining total energy values as discussed subsequently in connection with the radiation patterns. For three shots shown in Figure 22 (shots No. 13028, 13029, 13030), the corresponding P-wave energies (averaged from the observations at each gauge) are: 313, 231 and 143 $\times$ 10^5 ergs. The S-wave energies are 49.3, 3.72 and 0.73 $\times$ 10^5 ergs. The corresponding tensile prestress figures are 163, 163, and 114 bars. Note that the first two shots are in plexiglas and the third in pyrex glass.

The S-wave energies cannot come from the conversion of the explosive energy into S waves since very little if any S waves are generated by the explosions in unstressed plates. Thus, we must look into the energy release from the stressed plate. The explosion crushes a small circular region of the plate around the shot point. This normally does not exceed a radius of 1 cm. Beyond this region, some radial cracks extend to greater distances. If all of the strain energy in a zone of radius a_1 is radiated as seismic energy, the total amount will be

$$E_{ST} = [\pi a_1^2 h] \frac{1}{2} \sum_{i=1}^{3} \sigma_i \epsilon_i = \pi a_1^2 h \frac{2\bar{\sigma}^2}{E} \tag{12}$$

where E is Young's modulus and was determined from observed plate-wave velocities and h is the plate thickness. Equation (12) gives a good approximation to the upper limit of the available seismic energy if a_1 is taken to be the radius of the "quasi-elastic" cracked zone (Archambeau and Sammis, 1970). The problem that arises in estimating the energy from (12) is that of the definition of the cracked zone radius. In our experiments, the approximate values for the radius of the totally crushed and extensively cracked zone were about 0.4 cm and 1 cm, respectively. The values of E_{ST} for the strain levels of shots 13028, 13029 and 13030 are tabulated in Table 2 for the larger value of a (= 1 cm). Comparing these figures with the previously given wave energies, it will be apparent that the available strain energy is smaller than the total energy radiated as S waves for a = 1 cm.

We should further consider that not all of the available strain energy is radiated as seismic energy in the spectral range of our measurements, and this, too, must be divided into P and S waves. Thus, it is clear that a source region much larger than the crushed zone must be considered. This leads us to consider relaxation of the medium along the cracks that radiate to greater distances from the source than those considered in Table 2. The cracking phenomenon will be discussed below.

The second problem we must consider is the skewness of the P-wave radiation pattern. This phenomenon, apparent on our radiation patterns, can also be seen on the data of Kim and Kisslinger (1967). It cannot be attributed to asymmetry of the shot since it occurs only in the prestressed experiments. Since there is a contribution to P waves from the radiation of the strain energy due to the relaxation of the plate, then the mechanism of this relaxation must be taken into account. From the above discussion, as well as from the description of the cracking in the next section, the growth of the cracks does affect the radiation pattern. Furthermore, where cracks extend close to the observation position, the growth can be characterized as a unilateral tensile fault. This presumably is due to the scattering effect of the shattered region behind the crack tips on radiation not projected broadly in the direction of crack propagation.

TABLE 2

OBSERVED S WAVE AND CALCULATED MAXIMUM AVAILABLE ENERGIES FOR EXPLOSIONS IN PRESTRESSED PLEXIGLAS AND GLASS PLATES

Shot No.	Medium	Tensile Prestress (bars)	Observed S-Wave Energy (ergs)	Maximum Available Strain Energy (a = 1 cm) (ergs)
13028	Plexiglas	163	49.3×10^5	2.84×10^5
13029	Plexiglas	163 (?)	3.72×10^5	2.84×10^5
13030	Glass	114	0.73×10^5	0.16×10^5

We have computed the radiation pattern of a unilateral tensile fault propagating perpendicular to the tension axis, utilizing Ang and Williams' (1959) formulation as given by Savage and Mansinha (1963). The radiation patterns for P and S waves are proportional to

$$c(1 - 2V_S^2 \cos^2 \theta / V_P^2)/(V_P - c \cos \theta)$$

and

$$c \sin 2\theta/(V_S - c \cos \theta) \tag{13}$$

respectively, where c is the crack velocity. In our experiments, the observed radiation patterns of Figure 22 have an additional isotropic component due to the explosive source affecting the P-wave radiation patterns. A set of theoretical radiation patterns were calculated using (13) with the addition of various isotropic components. These are shown in Figure 23 for plexiglas.

Two aspects of Figure 23 are noteworthy. (a) Increasing crack propagation velocity produces a shift of the radiation pattern maximum in the direction of crack propagation, and (b) increasing the isotropic component, while broadening the radiation pattern, does not change the position of the maximum.

Inspecting the shift in the radiation pattern of P-waves from the observations of Figure 22 and comparing this to the theoretical shift, it is apparent that a crack velocity of 0.6 V_S is consistent with observations for both materials. In reducing the strain-gauge observations to wave energy, as listed in Table 2, gauge observations were corrected for the radiation pattern effects.

Near source phenomenon and crack propagation. The stresses in the immediate

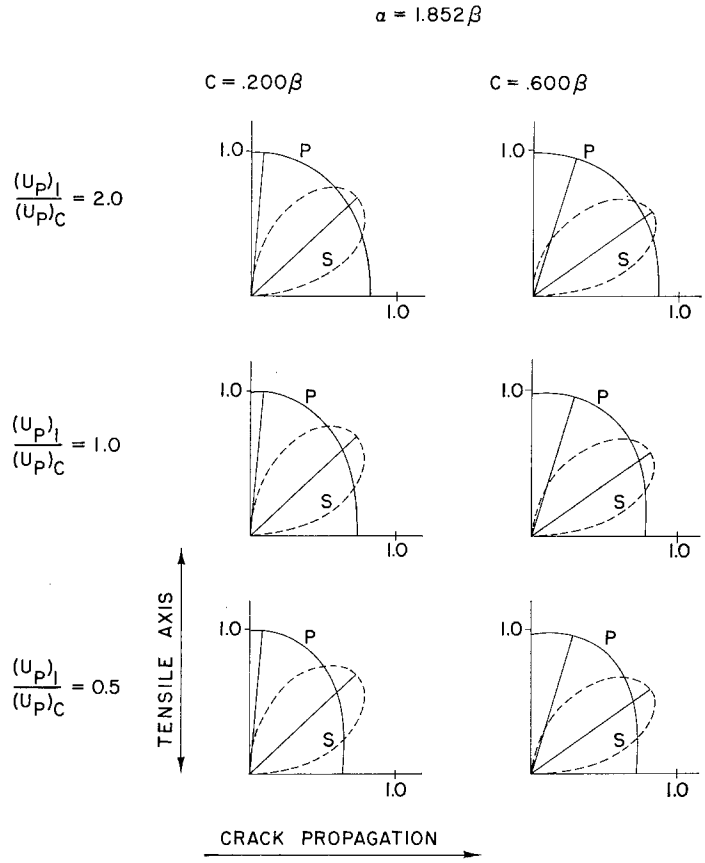

FIG. 23. Theoretical P- and S-wave radiation patterns from a tensile fault plus explosion in glass. Each *curve* is individually normalized to its extreme value. α, β are compressional and shear velocities in the plate. c = crack propagation velocity. U_P/U_{PC} is the ratio of the strength of the isotropic component to tensile crack component.

vicinity of the explosion are very high and may reach hundreds of kilobars. This easily exceeds the compressive strength of the material, and a crushed zone which extends from a few millimeters to a centimeter or more, depending on the shot size and the medium, is developed. As the stress wave propagates outward from the shot point, the pressure falls gradually until the elastic limit of the material is reached. Between the crushed and elastic zones, there is a region of radial cracking produced by the tensile failure during the unloading (dilatational) phase of the stress waves. Because of the importance of this region for the radiation patterns of seismic waves, great emphasis was placed on understanding its properties in our dynamic photoelastic experiments.

The immediate source region of an explosion in $\frac{1}{8}$-in-thick glass plate is shown in Figure 24. The evaporated zone (totally dark) and the crushed zone are indicated

very clearly. The initial radial cracks are visible along the inner edges of the isochromatics.

In unstressed plate experiments, the radial cracks are distributed isotropically and grow in radial directions. In the case of prestressed plates, initially the cracks do start radially. However, after some time, the cracks either stop growing or turn in the direction dictated by the stress axes. In the case of plates under tension, the favored direction of growth is perpendicular to the tension axis.

The propagation of explosion-induced cracks in glass plate under tension is shown in

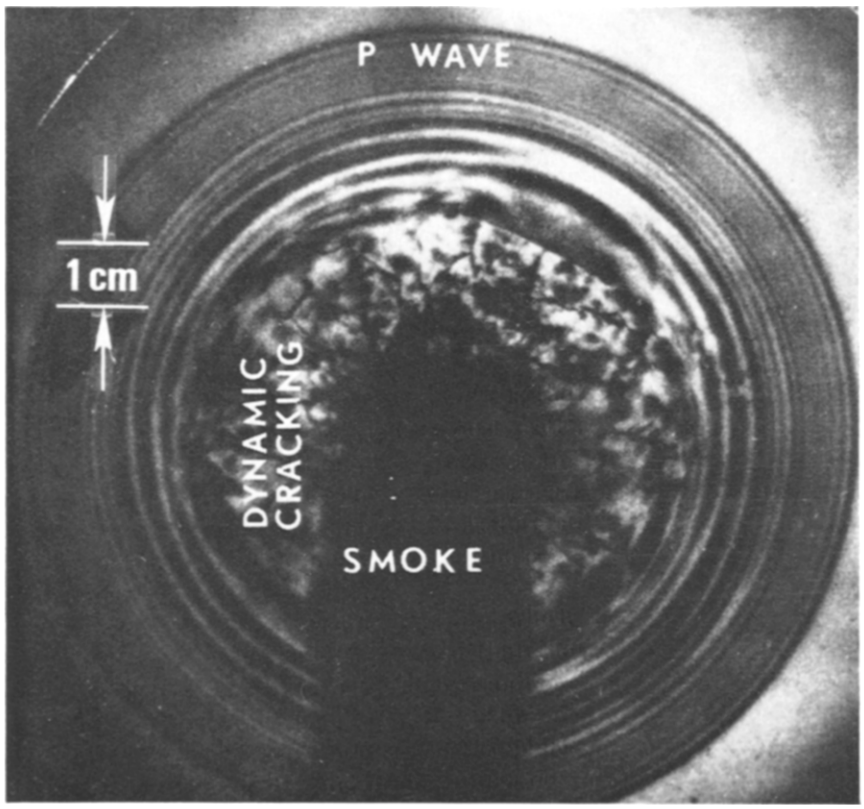

FIG. 24. Immediate source region of an explosive source in $\frac{1}{2}$-in thick pyrex plate glass, showing dynamic cracking and isochromatic fringe pattern. Picture taken 12 μsec after detonation. Exposure time is 0.1 μsec.

Figures 25, a, b, c, d. The preferred growth (in direction perpendicular to stress axis) and the radiation of seismic energy from the cracks (light zones) are indicated clearly. The stress concentration at crack tips is visible. The dark areas are the stress-free (relaxed) regions.

In addition to the above observations, we have been able to determine the velocity of the crack propagation by following the progress of crack tips in successive frames. By repeating this for shots at different stress levels, we have also been able to obtain the prestress dependence of the terminal velocity. The results for a glass plate are shown in Figure 26. First of all, the velocities indicated are terminal velocities. We could not determine the acceleration phase of the crack growth since our measurements could not begin before 2 cm radial distance. Secondly, there were variations in velocities between

c = 0.7 and 1.7 km/sec, when short as well as long cracks were measured. This range is indicated in Figure 26.

The highest crack velocity in unstressed glass plate is $c = 1.70 \pm 0.03$ km/sec. The ratios of this velocity to plate-compressional and shear velocities are $c/V_p = 0.32$

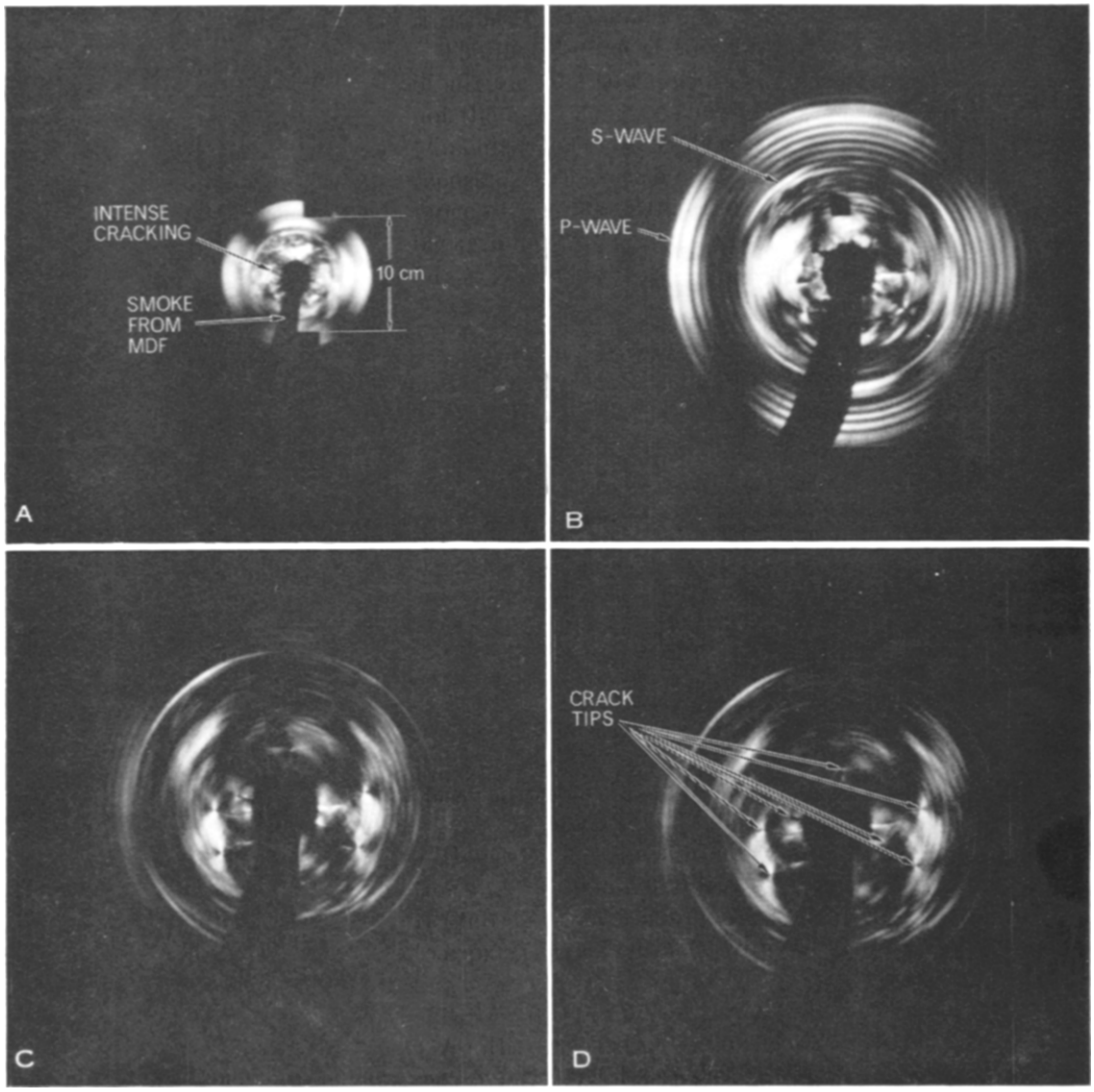

FIG. 25. Dynamic photoelastic isoclinic and isochromatic patterns produced by radial explosive source in $\frac{1}{8}$-in thick pyrex glass plate. Tensional prestress in vertical direction of 45 bars is applied to plate. Polarizer and analyzer polarization axes are at 45° and 135° with respect to horizontal. Effective exposure time for each frame is 0.25 μsec. A, B, C, and D frames were taken at 26.0, 42.7, 53.1, and 55.2 μsec after detonation.

and $c/V_s = 0.51$, respectively. For the glass plate stressed to 114 bars tension, the dynamic crack velocity was $c = 1.84 \pm 0.02$ km/sec and the ratios were $c/V_p = 0.35$ and $c/V_s = 0.55$. The intermediate (45 bar) tension prestress case gave values the same as the unstressed case within the experimental error.

It would be useful to compare our values of crack velocities with theoretical predic-

tion as well as other experimental results. There have been extensive theoretical studies of crack propagation (Liebowitz, Vols. I and II, 1968; Tetelman and McEvilly, 1967; and Cottrell, 1970). Very briefly, a necessary condition for the propagation of an elliptical elastic tensile crack is that the maximum tensile stress at its tip reach the theoretical cohesive strength. For completely brittle and elastic solids where the elastic limit is much greater than the cohesive stress, the Griffith relation can be applied. Considering the crack to be a thin ellipsoid with semi-major and minor axes l and h, the incremental release of the stored elastic strain energy (W_E) is equal to the incremental increase of surface energy (W_S) as new surface is created. At the tip of the crack, there is a strong stress concentration. The transfer of this elastic energy to moving the adjacent points apart at the crack tip limits the velocity of the crack growth. With these physical models, an expression can be derived for the propagation velocity of the crack (Tetelman and McEvilly, 1967)

$$c = 0.38\ V_p\left[1 - \frac{W_S}{W_E}\right]^{1/2} = 0.38\ V_p\left[\frac{1 - 8\mu(1+\nu)\gamma_S}{\pi\Sigma^2 l}\right]^{1/2} \tag{14}$$

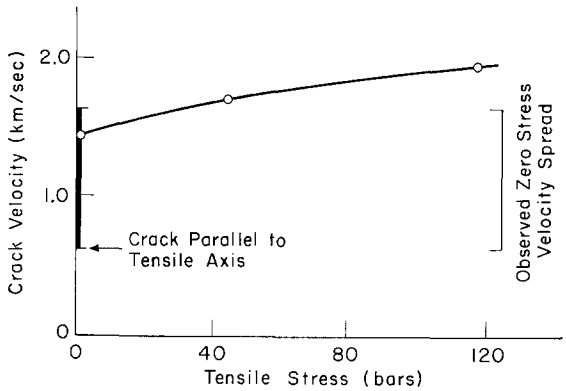

FIG. 26. Growth velocity of explosion-induced cracks in a glass plate. In unstressed plates there is a range of velocities depending on the crack length as shown above. In plates under tension, the crack growth is favored in directions perpendicular to the stress axis. Parallel to stress axis, velocity is low and cracks either stop growing or change direction.

where c = crack velocity, V_p = compressional velocity (plate velocity in our case) and W_s = surface energy of crack. W_E = strain energy in the crack, γ_s = unit surface energy and Σ = theoretical strength, l = half crack length and ν = Poisson's ratio. For soda-lime glasses, for example, approximate values are $\gamma_s \approx 10^3$ ergs/cm^2 and $\Sigma \approx 10^9$ dynes/cm^2 (Shand, 1961). From these, it is clear that the second term in the brackets is fairly small and the maximum theoretical crack velocity is $c = 0.38\ V_p$. This theoretical value is in agreement with some other predictions for tensile fractures in brittle material where a value of about $c = 0.63\ V_s$ is obtained (Yoffe, 1951; Mansinha, 1964). There have been other theoretical derivations relating the terminal crack velocity to Rayleigh velocity (Baker, 1962; Broberg, 1960; Craggs, 1960; Kachanov, 1961; Stroh, 1957). In these cases where crack velocity coincides with Rayleigh velocity, the theoretical values differ from others, unless the Rayleigh velocity is taken to be lower at the crack tip.

The effect of prestress in the material is to increase stress concentration and the strain energy W_E, while reducing the bonding energy W_s. Thus, as the prestress level increases, W_s/W_E approaches zero, and the crack velocity reaches its asymptotic value of $c \rightarrow 0.38\ V_p$.

The agreement between our measured values of crack velocity and the theoretical values of equation (14) is very good, both in absolute value and prestress dependence. The observed values are slightly lower than the theoretical values based on perfectly brittle behavior. This is expected since there is always some plastic deformation in the fracture process, and soft glasses always fail to reach the predicted terminal velocities.

There have been other measurements of crack velocities in glass (Schardin, 1959) and gabbro (Bieniawski, 1966) plates. These values are in excellent agreement with ours.

The implications of the explosion-induced crack growth in terms of the radiation pattern of seismic waves from underground explosions are significant. First of all, the cracking extends the source region, and also provides the means of converting some explosion energy into seismic waves of complicated radiation pattern. This radiation, however, is isotropic in the case of unstressed media. In the presence of a stress field or tectonic lineations, the cracks grow in a preferred direction and to greater lengths, resulting in coherent radiation of tectonic strain energy as well as some converted explosion energy. Even under ideal experimental conditions, however, some complexities are introduced into the radiation patterns due to the presence of several cracks, and irregularities in growth. These may explain the deviations of some data points from the idealized composite radiation patterns, in the case of field observations such as those of Figures 4 and 8.

Discussion and Conclusions

So far in this paper, we have described separately: (1) the source properties of several underground explosions as derived from the analysis of seismograms, and (2) the results of a series of laboratory experiments dealing with explosive sources in prestressed media. In this section, we will combine the results of both studies to explain the mechanisms of Love-wave generation and tectonic strain release by explosions.

The main results of field data analysis and the associated laboratory experiments are the following:

1. All explosions detonated in hard media (granite, rhyolite, tuff) generate some Love waves at or in the immediate vicinity of the source (see Table 1). Laboratory experiments indicate that the transverse waves are generated primarily because of the existence of a stress field. Even in brittle materials such as glass, under unstressed conditions, few transverse waves are generated by an explosive source compared to the prestressed case.

2. The Love- and Rayleigh-wave radiation patterns can be explained by a composite source consisting of an isotropic explosive source plus a double-couple source. It was assumed that the double-couple component was horizontal (pure strike-slip, vertical fault plane). With the available scattered data, it is not possible to determine uniquely and reliably more definite source models specifying all of the parameters (strike, dip angle, slip direction, magnitude) of the source function.

3. The strength of the double-couple source relative to the explosion (F value) increases with increasing strength of the medium as shown in Table 1. It should be remembered that: (a) F is period dependent, and the value listed in the Table 1 is applicable at $T \approx 15$ to 20 sec, and (b), in general, the F value listed is a lower bound since we assumed a vertical strike-slip source function for Love-wave generation. This is the most efficient radiator of Love waves, relative to Rayleigh waves. Any other double-couple source model that may fit the observed data would have a larger F value.

4. The orientation of the strike of the double couple, in general, is in agreement with

the strike of the tectonic fiber as determined from the existing faults, strikes of earthquakes, and the aftershocks following the large explosions such as BENHAM (Hamilton and Healy, 1969; Kehrer, 1969; McKeown and Dickey, 1969; Toksöz, *et al.*, 1965). This phenomenon is in agreement with what was observed in the experiments with an explosive point source in prestressed plates, where growth of the cracks and the radiation pattern of S waves were governed by the principal stresses.

5. The corrected spectra and the resulting time functions for the Love and Rayleigh waves showed that the Love-wave spectra were relatively richer at longer periods than Rayleigh-wave spectra. In fact, BILBY data as well as others indicate that the spectra of Love waves generated by the explosions are similar to those of comparable magnitude earthquakes. Explosion generated Rayleigh waves, on the other hand, have spectra shifted to shorter periods (Toksöz, *et al.*, 1965; Molnar, *et al.*, 1969; Toksöz, *et al.*, 1971). Our one-dimensional laboratory experiments also show that the time function of stress relaxation, generated in a prestressed rod, is of much lower frequency compared to those of the explosions (see Figure 15).

6. The energy of the double-couple component of the source holds the main clue to the source of this energy and the mechanism of its release. Although it is difficult to compute the total energy, at all frequencies, the power of the double-couple source relative to the explosion at $T \approx 20$ sec is proportional to F^2 (Table 1). The theoretical estimations of the strain energy release due to the introduction of a cavity in the prestressed medium are hampered by the lack of direct knowledge of prestress (Press and Archambeau, 1962; Toksöz *et al.*, 1965; Archambeau and Sammis, 1970; Smith *et al.*, 1969). The laboratory experiments provide some answers. From the strained rod experiments, we see that the S-wave strain amplitude increases linearly with prestress (Figure 16) as expected theoretically. The calculations carried out using data from unstressed plate experiments show that relaxation around the cavity alone cannot account for the radiated strain energy. This combined with the observed S-wave radiation patterns, requiring a growing crack, suggest that relaxation associated with extended cracking contributes significantly to the radiation of strain energy in prestressed media. In the case of field testing, relaxation of the medium occurs both along the newly-formed extended cracks (faults) and as movement along pre-existing fault zones. Strain measurements around the Nevada Test Site show this (Dickey, 1969).

7. Based on field studies as well as our laboratory experiments, we can state that explosions in prestressed media release some of the strain energy, and the mechanism of the release of this energy is similar to that of an earthquake. The amount of tectonic strain energy released depends strongly on the pre-existing stress level. Explosion-induced cracking controls the radiation pattern and the extent of tectonic strain energy release. The explosion cavity alone cannot account for all of the energy release. The radiation patterns of seismic waves are frequently complicated by the growth of cracks with finite velocities and relaxations along different faults and cracks.

Acknowledgments

This research was supported by the United States Air Force Office of Aerospace Research and monitored by Air Force Cambridge Research Laboratories under Contract F 19628-68-C-0043. The data from the BILBY explosion were analyzed at the Seismic Data Laboratory of Teledyne, Inc., supported by ARPA under the technical direction of AFTAC under contract F 33657-67-1313. The photoelastic work was performed at Stanford Research Institute and was supported by both the AFCRL and ARPA under contract Af 19(1628)-6048.

References

Aki, K. (1964). A note on surface wave generation from the Hardhat nuclear explosion, *J. Geophys. Res.* **69**, 1131–1134.

Alexander, S. S. (1963). Surface wave propagation in the Western United States, *Ph.D. Thesis*, California Institute of Technology, Pasadena, California.

Alverson, R. C. (1964). Spherical waves in elastic-plastic media, *Final Report on SRI Project No. GTU-3731*, Stanford Research Institute, Menlo Park, California, pp. 35–155.

Ang, D. D. and M. L. Williams (1959). Dynamic stress field due to an extensional dislocation, *Proc. Ann. Conf. on Solid Mech., 4th*, University of Texas, pp. 36–52.

Archambeau, C. B. (1968). General theory of elastodynamic source fields, *Rev. Geophys.* **6**, 241–288.

Archambeau, C. B. and C. Sammis (1970). Seismic radiation from explosions in prestressed media and the measurement of tectonic stress in the earth, *Rev. Geophys.* **8**, 473–499.

Baker, B. R. (1962). Dynamic stresses created by a moving crack, *J. Appl. Mech.* **29**, 449–458.

Barker, T. G., M. N. Toksöz, and R. W. Ward (1969). Explosion generated seismic waves, *AFCRL Report 69-0130*.

Ben-Menahem, A. and D. Harkrider, (1964). Radiation patterns of seismic surface waves from buried dipolar point sources in a flat stratified earth, *J. Geophys. Res.* **69**, 2605–2620.

Bieniawski, Z. T. (1966). Fracture velocity of rock, *Report MEG 517*, South African Council for Scientific and Industrial Research, Pretoria.

Bishop, R. H. (1963). Spherical shock waves from underground explosions: close-in phenomena of buried explosions, *Final Report, SC-4907(RR)*, Sandia Corporation, Albuquerque, pp. 115–158.

Broberg, K. B. (1960). The propagation of a brittle crack, *Arkiv Fysik* **18**, 159–192.

Brune, J. N. and P. W. Pomeroy (1963). Surface wave radiation patterns for underground nuclear explosions and small-magnitude earthquakes, *J. Geophys. Res.* **68**, 5005–5028.

Burridge, R. and L. Knopoff (1964). Body force equivalents for seismic dislocations, *Bull. Seism. Soc. Am.* **54**, 1875–1888.

Butkovich, T. R. (1965). Calculation of the shock wave from an underground nuclear explosion in granite, *J. Geophys. Res.* **70**, 885–892.

Cisternas, A. (1964). The radiation of elastic waves from a spherical cavity in a half-space, *Ph.D. Thesis*, California Institute of Technology, Pasadena, California.

Cottrell, A. H. (1970). The structure of a crack, in *Physics of Strength*, A. Argon, Editor, Massachusetts Institute of Technology Press, Cambridge, Massachusetts (in press).

Craggs, J. W. (1960). On the propagation of a crack in an elastic-brittle material, *J. Mech. Phys. Solids*, **8**, 66.

Dickey, D. D. (1969). Strain associated with the Benham underground nuclear explosion, *Bull. Seism. Soc. Am.* **59**, 2221–2230.

Hamilton, R. M. and J. H. Healy (1969). Aftershocks of the Benham nuclear explosion, *Bull. Seism. Soc. Am.* **59**, 2271–2281.

Harkrider, D. G. (1964). Surface waves in multilayered elastic media, 1, Rayleigh and Love waves from buried sources in a multilayered elastic half-space, *Bull. Seism. Soc. Am.* **54**, 627–680.

Honda, H. (1962). Earthquake mechanism and seismic waves, *Geophys. Notes* **15**, 1–97 (supplement).

Kachanov, L. M. (1971). On kinetics of crack growth, PMM, *Zh. Prikl. Mat. i Mekhan., Moskow* **25**, 498–502, (in Russian).

Kehrer, H. H. (1969). Radiation patterns of seismic surface waves from nuclear explosions, *M.S. Thesis*, Massachusetts Institute of Technology, Cambridge, Massachusetts.

Kim, W. H. and C. Kisslinger (1967). Model investigations of explosions in prestressed media, *Geophysics* **32**, 633–651.

Kisslinger, C., E. J. Mateker, and T. V. McEvilly (1961). SH motion from explosions in soil, *J. Geophys. Res.* **66**, 3487–3496.

Kisslinger, C. and I. N. Gupta (1963). Studies of explosion-generated dilatational waves in two-dimensional models, *J. Geophys. Res.* **68**, 5197–5206.

Kromm, A. (1948). The propagation of elastic waves in plane discs with a circular hole, *Z. Angew. Math. Mech.*, **28**, 104–114.

Liebowitz, H. (editor) (1968). *Fracture, an advanced treatise*, Vol. 1 and 2, Academic Press, New York.

Mansinha, L. (1964). The velocity of shear fracture, *Bull. Seism. Soc. Am.* **54**, 369–376.

McKeown, F. A. and D. D. Dickey (1969). Fault displacements and motion related to nuclear explosions, *Bull. Seism. Soc. Am.*, **59**, 2253–2269.

Molnar, P., K. Jocob, and L. R. Sykes (1969). Microearthquake activity in eastern Nevada and Death Valley, California, before and after the nuclear explosion Benham, *Bull. Seism. Soc. Am.* **59**, 2177–2184.

Perrett, William R. (1968). Free field particle motion from a nuclear explosion in salt, Part I, *VUF 3012*, Sandia Laboratory.

Press, F. and C. B. Archambeau (1962). Release of tectonic strain by underground nuclear explosions, *J. Geophys. Res.* **67**, 337–343.

Savage, J. C. and L. Mansinha (1963). Radiation from a tensile fracture, *J. Geophys. Res.* **68**, 6345–6358.

Savin, G. N. (1966). *Stress concentration around holes*, Pergamon Press, New York.

Schardin, H. (1959). *Fracture*, B. L. Auerbach, D. K. Fellbeck, G. T. Hahn, and D. A. Thomas, Editors, Wiley, New York.

Shand, E. B. (1961). Fracture velocity and fracture energy of glass in the fatigue range, *J. Am. Ceram. Soc.* **44**, 21–26.

Smith S. W. (1963). Generation of seismic waves by underground explosions and the collapse of cavities, *J. Geophys. Res.* **68**, 1477–1483.

Smith, S. W., C. B. Archambeau, and W. Gile (1969). Transient and residual strains from large underground explosions, *Bull. Seism. Soc. Am.* **59**, 2185–2196.

Stroh, A. N. (1957). A theory of the fracture of metals, *Advan. Phys.* **6**, 418–465.

Tetelman, A. S. and A. J. McEvilly, Jr. (1967). *Fracture of structural materials*, Wiley, New York.

Thomson, K. C., T. J. Ahrens, and M. N. Toksöz (1969). Dynamic Photoelastic studies of *P* and *S* wave propagation in prestressed media, *Geophysics* **34**, 696–712.

Toksöz, M. N. (1967). Radiation of seismic surface waves from underground explosions, *Proceedings of the Vesiac Conference on the current status and future prognosis of shallow seismic events*, *VESIAC Rept.*, Willow Run Laboratories, The University of Michigan, pp. 65–84.

Toksöz, M. N. and K. Clermont (1967). Radiation of seismic waves from the Bilby explosion, *Seismic Data Laboratory Technical Report 183*, prepared for AFTAC, Teledyne, Inc.

Toksöz, M. N., A. Ben-Menahem, and D. G. Harkrider (1964). Determination of source parameters by amplitude equalization of seismic surface waves, 1. Underground nuclear explosions, *J. Geophys. Res.* **69**, 4355–4366.

Toksöz, M. N., D. G. Harkrider, and A. Ben-Menahem (1965). Determination of source parameters by amplitude equalization of seismic surface waves, 2. Release of tectonic strain by underground nuclear explosions and mechanisms of earthquakes, *J. Geophys. Res.* **70**, 907–922.

Toksöz, M. N., H. Kehrer, and R. Ward (1971). Source properties of NTS explosions (in preparation).

Tsai, Y. B. and K. Aki (1971). Amplitude spectra of surface waves from small earthquakes and underground nuclear explosions, *J. Geophys. Res.* **76**, 3940–3952.

Wistor, J. W., J. A. Beyeler, and G. J. Hansen (1963). Long-period displacement gages: close-in phenomena of buried explosions, *Final Report SC-4907 (RR)*, Sandia Corp., Albuquerque, 57–82.

Yoffe, E. H. (1951). The moving Griffith crack, *Phil. Mag.*, **42**, 739–750.

Zvolinskii, N. V. (1960). On the emission of an elastic wave from a spherical explosion in the ground, *Soviet J. Appl. Math. Mech.* **24**, 166–176.

Department of Earth and
Planetary Sciences
Massachusetts Institute
of Technology
Cambridge, Massachusetts 02139 (M.N.T.)

Air Force Cambridge
Research Laboratories
Laurence G. Hanscom Field
Bedford, Massachusetts 01730 (K.C.T.)

Seismological Laboratory
California Institute
of Technology
Pasadena, California 91109 (T.J.A.)

Division of Geological and Planetary
Sciences
California Institute of Technology
Contribution No. 20000

Manuscript received April 5, 1971